

presence of alveolitis and the subsequent destruction of the alveolar–blood interface related to sarcoidosis may influence KL-6/MUC1 efflux from the alveoli into the bloodstream. The effects of local production of KL-6/MUC1 by regenerating type II epithelial cells on this efflux also need to be considered in some subjects.

Thus, performing an analysis in healthy subjects is crucial for understanding the association between serum KL-6 concentration and ILDs. Therefore, in this study, we focused only on healthy subjects and evaluated the associations between MUC1 allele-related molecular sizes and efflux behavior of KL-6/MUC1, as well as factors contributing to efflux behavior and serum KL-6 concentrations.

2. Materials and methods

2.1. Subjects

A total of 250 unrelated healthy Japanese subjects, who visited for routine physical examination, were enrolled into this study. By completing a questionnaire, these subjects provided relevant background information, including medication use, and hereditary diseases. We excluded subjects who met the following conditions: (1) history of any pulmonary disease or respiratory symptoms; (2) percent of predicted vital capacity $\leq 80\%$; (3) ratio of forced expiratory volume in the first 1 s to the forced vital capacity of the lungs $\leq 70\%$; and (4) estimated glomerular filtration rate (eGFR) ≤ 60 ml/min/1.73 m². eGFR was calculated using the following equation for Japanese populations [14]: $eGFR = 194 \times \text{serum creatinine}^{-1.094} \times \text{Age}^{-0.287}$ (for females, $\times 0.739$). To definitively evaluate the effects of cigarette smoking on the efflux behavior of KL-6/MUC1 and serum KL-6 concentrations, we excluded former smokers from this study. The study population, gender, age, smoking history, serum KL-6 concentrations and eGFR levels are shown in Table 1.

Venous blood samples were collected into Vacutainer™ tubes containing clot activator, and were kept in the tubes for 30 min. Tubes were centrifuged at 3000 rpm at room temperature for 10 min. Serum samples were immediately frozen and stored at -80°C until assay. The Institutional Review Board of the School of Medicine, Hokkaido University, approved the study protocols and all subjects provided formal written consent.

2.2. Genotyping of MUC1 polymorphism

The MUC1 SNP (exon 2; rs4072037) was genotyped using the TaqMan system (Assay ID: C_27532642_10; Applied Biosystems, Foster City, CA).

2.3. Western blotting

Western blotting was performed on all serum samples as described previously [13]. Briefly, protein samples from serum were electrophoresed on 3%–8% NUPAGE Tris-acetate gels (Invitrogen, Carlsbad, CA) and were transferred to nitrocellulose membranes

(Invitrogen). Membranes were blocked with PBS containing 3% skim milk. Western blot analysis was performed using anti-KL-6 antibody (anti-KL-6 antibody was kindly provided by Sanko Junyaku Co., Ltd., Tokyo, Japan) followed by alkaline phosphatase-conjugated goat anti-mouse Ig. Bands were developed using the Western Breeze Chromogenic Immunodetection Kit (Invitrogen).

2.4. Measurements of KL-6 and creatinine

KL-6 concentrations in serum were measured by electrochemiluminescent immunoassay using the PICOLUMI KL-6 kit (Sanko Junyaku). Concentrations of creatinine in serum were measured using a Hitachi 7170 automated analyzer with Serotec CRE-L (Serotec, Sapporo, Japan) standardized using the isotopic dilution mass spectrometry method.

2.5. Statistical methods

Statistical analysis was performed with SPSS for Windows (SPSS Inc., Chicago, IL). Data are expressed as medians and ranges. All data were not normally distributed on univariate analysis, and the natural logarithms of all data were used for further statistical analyses. Comparisons were performed using unpaired *t*-test. Differences between groups were evaluated by ANOVA and were assessed by Bonferroni post-hoc test. Correlations between different parameters were determined by Pearson's correlation coefficient. We used Haploview software ver 4.1 (<http://www.broad.mit.edu/mpg/haploview>) in order to compare the observed numbers of genotypes with the number of expected genotypes under the Hardy–Weinberg equilibrium using the χ^2 -test. The relationship between efflux behavior of high molecular size KL-6/MUC1 and smoking status was assessed using χ^2 -test. A *p* ≤ 0.05 was regarded as significant.

3. Results

3.1. MUC1 genotypes and Western blot analysis

There were 448 (89.6%) sequences with A and 52 (10.4%) with G. The genotype frequencies were 204 (81.6%) for AA, 40 (16.0%) for AG, and 6 (2.4%) for GG. No significant deviation from the Hardy–Weinberg equilibrium was observed (*p* > 0.05). Western blot analysis of serum with anti-KL-6 antibody revealed 3 bands (low molecular size (L), middle molecular size (M) and high molecular size (H), at approximately 400, 450 and 500 kDa, respectively) and four band patterns (L alone, LM, LH and H alone) under reducing conditions, as described previously [13]. The frequency and percentage of the MUC1 genotypes and the KL-6/MUC1 band patterns in serum are summarized in Table 2.

In our previous report, we demonstrated a significant relationship between MUC1 genotypes and KL-6/MUC1 molecular sizes in BALF in 128 subjects with sarcoidosis; the A allele was linked with the low molecular size KL-6/MUC1 and the G allele with the high molecular size [13]. Therefore, we can extrapolate the KL-6/MUC1 molecular sizes in BALF from the subjects in this study according to MUC1 genotypes. Namely, the subjects with genotype AA correspond to low molecular size band patterns (i.e. L alone) in BALF and the subjects with genotype non-AA correspond to higher molecular size band patterns (i.e. LM, LH and H alone). Next, we examined the association between MUC1 genotypes (molecular size of KL-6/MUC1 in BALF) and KL-6/MUC1 band pattern in serum. In the subjects with genotype AA (i.e. low molecular size band patterns in BALF), all subjects displayed L alone bands in serum. On the other hand, the subjects with genotype non-AA (i.e. higher molecular size band patterns in BALF) showed diverse patterns in serum.

Based on the presence of higher molecular size bands (M or H) in serum (i.e., the efflux of higher molecular size KL-6/MUC1 from the alveoli to the bloodstream), we classified the subjects with genotype non-AA into two groups according to the absence or presence of higher

Table 1
Characteristics of the study population.

	Healthy subjects
No. of subjects	250
Men/women	113/137
Age, y	51 (24–77)
Cigarette smoking	
Never/current	157/93
MUC1 gene polymorphism	
AA/AG/GG	204/40/6
Serum KL-6 concentrations, U/ml	214 (112–759)
eGFR levels, ml/min/1.73 m ²	84.6 (60.3–268.7)

Data are presented as median (range).

Table 2
The relationship between MUC1 genotypes and KL-6/MUC1 band patterns in serum.

		Band patterns in serum				Total
		L-alone	LM, LH	H alone	Not detected	
rs4072037	AA	190			14	204
		93.1%			6.9%	100.0%
	AG	32	6		2	40
		80.0%	15.0%		5.0%	100.0%
	GG			1	5	6
				16.7%	83.3%	100.0%
Total		222	6	1	21	250
		88.8%	2.4%	0.4%	8.4%	100.0%

molecular size bands (M or H) in serum, “non-efflux” and “efflux”. The non-efflux group displayed only L bands (neither M nor H bands) in serum. In contrast, the efflux group displayed M or H bands in addition to L bands. Thirty-two of forty-six subjects with higher molecular size band patterns in BALF (84.8%) were classified as “non-efflux” and 7 of 46 subjects (15.2%) were classified as “efflux”.

3.2. Serum KL-6 concentrations in healthy subjects

Clinical characteristics and serum KL-6 data are shown in Table 1. The median age was 51 y (range, 24–77 y). There were significantly more smokers among male subjects than among female subjects (χ^2 -test, $p < 0.001$). The median concentration of serum KL-6 in all healthy subjects was 214 U/ml (range, 112–759 U/ml). Serum KL-6 concentrations in current smokers were significantly higher than those in never smokers ($p < 0.001$). A significant positive correlation was observed between serum KL-6 concentrations and age ($r = 0.327$, $p < 0.001$). A significant negative correlation was observed between concentrations of serum KL-6 and eGFR ($r = -0.213$, $p = 0.001$). Next, serum KL-6 concentrations were analyzed for each MUC1 genotype. The median concentrations of serum KL-6 in subjects with genotypes AA, AG and GG were 202, 307 and 425 U/ml, respectively. Serum KL-6 concentrations in subjects with genotypes AG and GG (i.e., higher molecular size KL-6/MUC1 in BALF) were significantly higher than in those with genotype AA

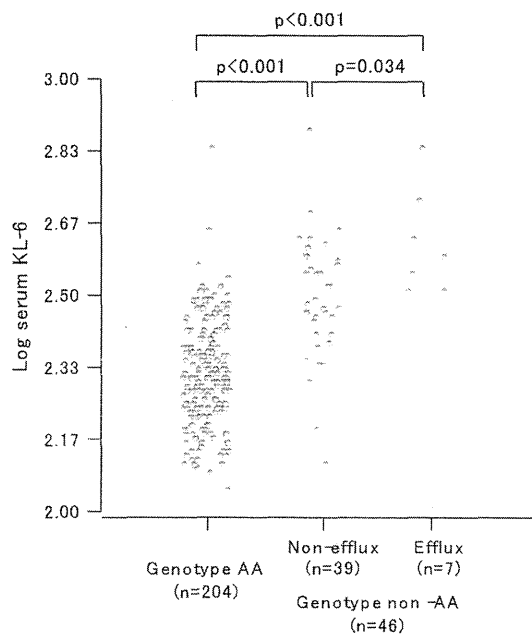


Fig. 1. Serum KL-6 concentrations in each genotype based on band patterns in serum.

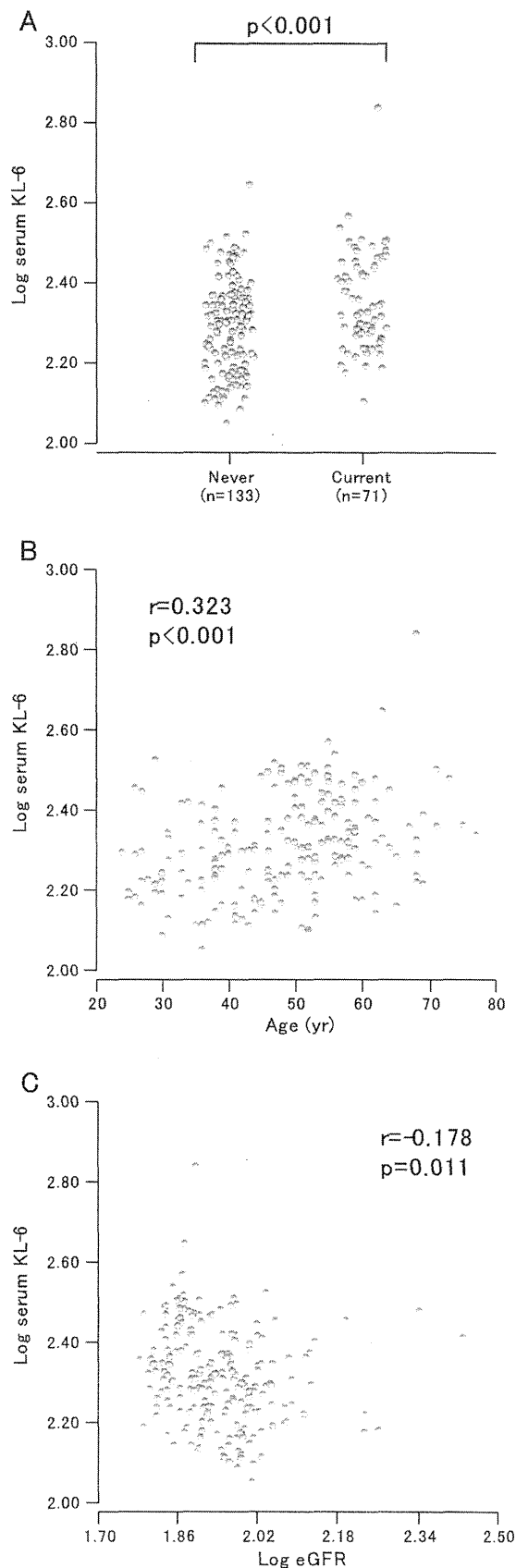
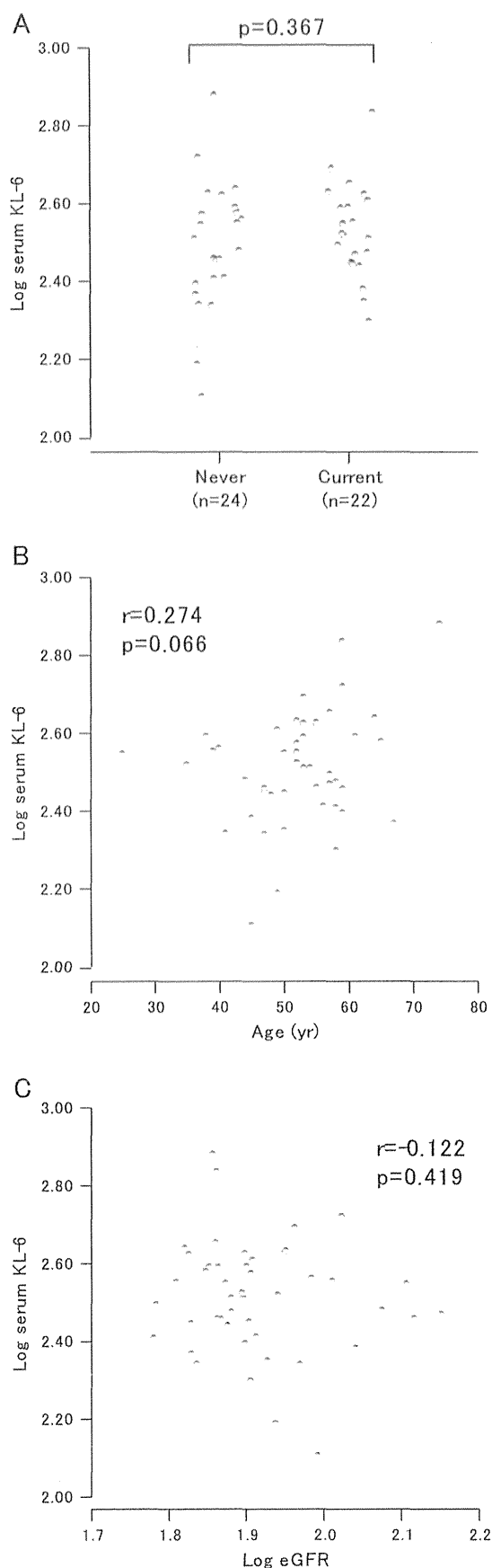


Fig. 2. Relationships between serum KL-6 concentrations and smoking status, age and renal function in subjects with genotype AA (i.e., low molecular size KL-6/MUC1 in BALF). A, vs. smoking status; B, vs. age and C, vs. eGFR levels.



(i.e., low molecular size KL-6/MUC1 in BALF) ($p < 0.001$ and $p < 0.001$, respectively).

3.3. Impact of KL-6/MUC1 molecular size on serum KL-6 concentrations in healthy subjects

When serum KL-6 concentrations were analyzed for each genotype based on band pattern in serum, serum KL-6 concentrations in both the non-efflux (i.e., L-alone) and efflux groups (i.e., LM, LM or H/H) from the subjects with genotype non-AA were significantly higher than those in subjects with genotype AA (i.e., L-alone) ($p < 0.001$ and $p < 0.001$, respectively, Fig. 1). In subjects with genotype non-AA, serum KL-6 concentrations in the efflux group were significantly higher than those in the non-efflux group ($p = 0.034$, Fig. 1).

Among subjects with genotype AA (i.e., low molecular size KL-6/MUC1 in BALF), serum KL-6 concentrations in current smokers were significantly higher than those in never smokers ($p < 0.001$) (Fig. 2A). A significant positive correlation was observed between serum KL-6 concentrations and age ($r = 0.323$, $p < 0.001$) (Fig. 2B). A significant negative correlation was observed between the concentrations of serum KL-6 and eGFR ($r = -0.178$, $p = 0.011$) (Fig. 2C).

In subjects with genotype non-AA (i.e., higher molecular size KL-6/MUC1 in BALF), there were no significant differences in serum KL-6 concentrations between current and never smokers ($p = 0.367$, Fig. 3A). In addition, no significant correlations between serum KL-6 concentrations, and age and eGFR levels were observed ($r = 0.274$, $p = 0.066$ and $r = -0.122$, $p = 0.419$, respectively, Fig. 3B and C). Next, we examined the effects of cigarette smoking, aging and renal function on the efflux behavior of high molecular size KL-6/MUC1. The efflux behavior of higher molecular size KL-6/MUC1 appeared to be affected by cigarette smoking in some subjects, but did not reach statistical significance (χ^2 -test, $p = 0.680$) (Table 3). No significant differences were observed in aging and renal function between the non-efflux and efflux groups ($p = 0.327$ and 0.835 , respectively).

4. Discussion

The KL-6/MUC1 efflux from the alveoli into the bloodstream depends on the increased permeability, following destruction of the alveolar–blood interface [7,8]. In addition to this mechanism, we have recently discovered that the efflux mechanism of KL-6/MUC1 differed according to MUC1 allele related molecular sizes in sarcoidosis [13]. In this study, based on an analysis of healthy subjects, we demonstrated 3 important findings with regard to the KL-6/MUC1 efflux based on molecular structural variants. First, high molecular size KL-6/MUC1 was detected in the serum of some subjects. Thus, high molecular size KL-6/MUC1 was able to pass through the alveolar–blood interface even in healthy subjects. Second, the effects of cigarette smoking and aging on the efflux behavior of KL-6/MUC1 differed according to KL-6/MUC1 molecular size. Finally, the efflux behavior of high molecular size KL-6/MUC1 was a significant determinant of serum KL-6 concentrations in subjects with high molecular size KL-6/MUC1.

The major allele frequency of rs4072037 differs with ethnicity. According to the HapMap database, “A” allele frequency is much higher than “G” allele in the Japanese population, which is consistent with our observed frequency. The distributions of the rs4072037 genotypes did not differ between healthy subjects and patients with sarcoidosis [13] in our studies.

Fig. 3. Relationships between serum KL-6 concentrations and smoking status, age, renal function and efflux behavior of high molecular size KL-6/MUC1 in subjects with genotype non-AA (i.e. higher molecular size KL-6/MUC1 in BALF). A, vs. smoking status; B, vs. age; C, vs. eGFR levels.

Table 3
Relationship between efflux behavior of higher molecular size KL-6/MUC1 and smoking status.

		Efflux behavior of high molecular size KL-6/MUC1		Total
		Non-efflux	Efflux	
Smoking status	Never	20 83.8%	4 16.7%	24 100.0%
	Current	19 86.4%	3 13.6%	22 100.0%
Total		39 84.8%	7 15.2%	46 100.0%

χ^2 -test, $p = 0.680$.

The KL-6/MUC1 efflux mechanism from the alveoli into the bloodstream is complex. In this study, there were significant relationships between increased serum KL-6 concentrations, and smoking status and aging in subjects with low molecular size KL-6/MUC1 (i.e., genotype AA). Cigarette smoke exposure is known to increase the permeability of the lung epithelial/endothelial barrier [15,16]. Previous reports have suggested that age-related changes in healthy subjects are associated with increased permeability of KL-6/MUC1 [9,11]. The efflux of low molecular size KL-6/MUC1 would be induced by cigarette smoking and aging in healthy subjects. With regard to the efflux behavior of high molecular size KL-6/MUC1 in subjects with higher molecular size KL-6/MUC1 (i.e., genotype non-AA), 7 of 46 subjects (15.2%) exhibited an efflux of higher molecular size KL-6/MUC1 into blood. Although this percentage is lower than in subjects with sarcoidosis (34.0%) [13], this finding suggests that the high molecular size KL-6/MUC1 is able to pass through the alveolar–blood interface, even in healthy subjects. Furthermore, we evaluated the association of cigarette smoking and aging with the efflux behavior of high molecular size KL-6/MUC1. These factors appeared to have little influence on efflux behavior. The exact factors contributing to the efflux of high molecular size KL-6/MUC1 could not be determined in the present study. As discussed previously [13], the efflux mechanism of high molecular size KL-6/MUC1 may be regulated by individual pore size and/or electrostatic forces at the alveolar blood interface, and this requires further clarification in the future.

It should be also noted that factors contributing to serum KL-6 concentrations in healthy subjects differed according to the KL-6/MUC1 molecular size. In subjects with low molecular size KL-6/MUC1 (i.e., genotype AA), our findings related to cigarette smoking and aging were consistent with previous findings [9,11]. In addition, we identified a significant association between serum KL-6 concentrations and renal function. The possible association between increased KL-6 excretion in the renal tubulus and increased urinary KL-6 concentrations has been discussed previously [10]. Renal function should also be considered for the interpretation of serum KL-6 concentrations in these subjects. In contrast, in subjects with higher molecular size KL-6/MUC1 (i.e., genotype non-AA), cigarette smoking, aging and renal function were not associated with serum KL-6 concentrations. The efflux behavior of higher molecular size KL-6/MUC1 was a significant factor contributing to the increased concentrations of serum KL-6. These results suggest that the impact of efflux behavior on serum KL-6 concentrations is greater than those of other factors such as cigarette smoking, aging and renal function. Therefore, the efflux behavior of high molecular size KL-6/MUC1 should be considered when interpreting serum KL-6 concentrations in healthy subjects, particularly with the high molecular size KL-6/MUC1.

There are significant limitations with regard to Western blotting in this study. Specifically, Western blotting was not performed on BALF samples. However, we analyzed genetic polymorphisms of the MUC1 gene (rs4072037) in all subjects. Based on our previous report

[13], rs4072037 genotypes are strongly linked to KL-6/MUC1 molecular sizes found in BALF. Therefore, KL-6/MUC1 molecular sizes in BALF could be extrapolated based on rs4072037 genotypes, although other MUC1 SNPs might be also associated with KL-6/MUC1 molecular sizes in BALF. Serum KL-6 concentrations in the non-efflux group, which included “not detected” subjects, from the subjects with genotype non-AA were significantly higher than those in the subjects with genotype AA. This indicates that efflux of high molecular size KL-6/MUC1 at the alveolar–blood interface is likely to occur, even in these subjects, to an undetectable degree on Western blot analysis. High sensitivity quantitative analysis for each molecular size of KL-6/MUC1 may still be important for understanding the efflux mechanisms of KL-6/MUC1.

5. Conclusions

This study showed an association between KL-6/MUC1 efflux based on genetically determined molecular sizes of KL-6/MUC1 and serum KL-6 concentrations in healthy subjects. We propose that the molecular size and efflux behavior of KL-6/MUC1 should be considered when interpreting serum KL-6 data. Taken together with the results of our previous study, this information will assist in the interpretation of serum KL-6 data in both healthy subjects and subjects with ILDs.

References

- [1] Kohno N, Akiyama M, Kyoizumi S, Hakoda M, Kohuke K, Yamakido M. Detection of soluble tumor-associated antigens in sera and effusions using novel monoclonal antibodies, KL-3 and KL-6, against lung adenocarcinoma. *Jpn J Clin Oncol* 1988;18:203–16.
- [2] Hirasawa Y, Kohno N, Yokoyama A, Inoue Y, Abe M, Hiwada K. KL-6, a human MUC1 mucin, is chemotactic for human fibroblasts. *Am J Respir Cell Mol Biol* 1997;17:501–7.
- [3] Kohno N, Awaya Y, Oyama T, et al. KL-6, a mucin-like glycoprotein, in bronchoalveolar lavage fluid from patients with interstitial lung disease. *Am Rev Respir Dis* 1993;148:637–42.
- [4] Ohnishi H, Yokoyama A, Yasuhara Y, et al. Circulating KL-6 levels in patients with drug induced pneumonitis. *Thorax* 2003;58:872–5.
- [5] Sakamoto K, Taniguchi H, Kandoh Y, et al. Serum KL-6 in fibrotic NSIP: correlations with physiologic and radiologic parameters. *Respir Med* 2010;104:127–33.
- [6] Miyoshi S, Hamada H, Kadowaki T, et al. Comparative evaluation of serum markers in pulmonary sarcoidosis. *Chest* 2010;137:1391–7.
- [7] Inoue Y, Barker E, Daniloff B, Kohno N, Hiwada K, Newman LS. Pulmonary epithelial cell injury and alveolar–capillary permeability in berylliosis. *Am J Respir Crit Care Med* 1997;156:109–15.
- [8] Ohtsuki Y, Fujita J, Hachisuka Y, et al. Immunohistochemical and immunoelectron microscopic studies of the localization of KL-6 and epithelial membrane antigen (EMA) in presumably normal pulmonary tissue and in interstitial pneumonia. *Med Mol Morphol* 2007;40:198–202.
- [9] Ishikawa N, Mazur W, Toljam O, et al. Ageing and long-term smoking affects KL-6 levels in the lung, induced sputum and plasma. *BMC Pulm Med* 2011;11:22.
- [10] Narita J, Hasegawa T, Tsuchida M, et al. Analysis of the effect of surgical lung biopsy on serum KL-6 levels in patients with interstitial pneumonia: surgical lung biopsy does not elevate serum KL-6 levels. *Intern Med* 2006;45:615–9.
- [11] Janssen R, Kruit A, Grutters JC, Ruven HJ, Gerritsen WB, van den Bosch JM. The mucin-1 568 adenosine to guanine polymorphism influences serum Krebs von den Lungen-6 levels. *Am J Respir Cell Mol Biol* 2006;34:496–9.
- [12] Horimatsu Y, Hattori N, Ishikawa N, et al. Different MUC1 gene polymorphisms in German and Japanese ethnicities affect serum KL-6 levels. *Respir Med* 2012;106:1756–61.
- [13] Shigemura M, Nasuhara Y, Konno S, et al. Effects of molecular structural variants on serum Krebs von den Lungen-6 levels in sarcoidosis. *J Transl Med* 2012;10:111.
- [14] Matsuo S, Imai E, Horio M, et al. Revised equations for estimated GFR from serum creatinine in Japan. *Am J Kidney Dis* 2009;53:982–92.
- [15] Jones JG, Minty BD, Lawler P, Hulands G, Crawley JC, Veall N. Increased alveolar epithelial permeability in cigarette smokers. *Lancet* 1980;1:66–8.
- [16] Rusznak C, Mills PR, Devalia JL, Sapsford RJ, Davies RJ, Lozewicz S. Effect of cigarette smoke on the permeability and H-1beta and sICAM-1 release from cultured human bronchial epithelial cells of never-smokers, smokers, and patients with chronic obstructive pulmonary disease. *Am J Respir Cell Mol Biol* 2000;23:530–6.

Cross-sectional and prospective study of the association between lung function and prediabetes

Takashi Yamane,^{1,2} Akihito Yokoyama,¹ Yoshihiro Kitahara,² Shintaro Miyamoto,¹ Yoshinori Haruta,² Noboru Hattori,² Kiminori Yamane,^{2,3} Hitoshi Hara,³ Nobuoki Kohno²

To cite: Yamane T, Yokoyama A, Kitahara Y, *et al*. Cross-sectional and prospective study of the association between lung function and prediabetes. *BMJ Open* 2013;**3**:e002179. doi:10.1136/bmjopen-2012-002179

► Prepublication history for this paper are available online. To view these files please visit the journal online (<http://dx.doi.org/10.1136/bmjopen-2012-002179>).

Received 12 October 2012
Revised 10 December 2012
Accepted 21 January 2013

This final article is available for use under the terms of the Creative Commons Attribution Non-Commercial 2.0 Licence; see <http://bmjopen.bmj.com>

¹Department of Hematology and Respiratory Medicine, Kochi University, Kochi, Japan

²Department of Molecular and Internal Medicine, Hiroshima University, Hiroshima, Japan

³Nippon Telegraph and Telephone West Corporation Chugoku Health Administration Center, Hiroshima, Japan

Correspondence to Professor Akihito Yokoyama; ayokoyama@kochi-u.ac.jp

ABSTRACT

Objectives: A growing body of evidence suggests that there is a relationship between impaired lung function and the risk of developing diabetes mellitus (DM). However, it is not known if this reflects a causal effect of lung function on glucose metabolism. To clarify the relationship between lung function and the development of DM, we examined the incidence of newly diagnosed prediabetes (a precursor of DM) among subjects with normal glucose tolerance (NGT) at baseline.

Design: Primary analysis of an occupational cohort with both cross-sectional and longitudinal data (follow-up duration mean±SD: 28.4±6.1 months).

Setting and participants: Data were analysed from 1058 men in a cross-sectional study and from 560 men with NGT in a longitudinal study.

Outcomes and methods: Impaired lung function (per cent predicted value of forced vital capacity (%FVC) or per cent value of forced expiratory volume 1 s/FVC (FEV₁/FVC ratio)) in relation to the ratio of prediabetes or DM in a cross-sectional study and development of new prediabetes in a longitudinal study. NGT, prediabetes including impaired glucose tolerance (IGT) and increased fasting glucose (IFG) and DM were diagnosed according to 75 g oral glucose tolerance tests.

Measurements and main results: %FVC at baseline, but not FEV₁/FVC ratio at baseline, was significantly associated with the incidences of DM and prediabetes. Among prediabetes, IGT but not IFG was associated with %FVC. During follow-up, 102 subjects developed prediabetes among those with NGT. A low %FVC, but not FEV₁/FVC ratio, was predictive of an increased risk for development of IGT, but not of IFG.

Conclusions: Low lung volume is associated with an increased risk for the development of prediabetes, especially IGT, in Japanese men. Although there is published evidence for an association between chronic obstructive pulmonary disease and DM, prediabetes is not associated with the early stage of COPD.

INTRODUCTION

Accumulating evidence suggests that there is a close relationship between impaired lung

ARTICLE SUMMARY

Article focus

■ We hypothesised that lung function is associated with the development of impaired glucose metabolism. To investigate this, the data of an occupational cohort were analysed from 1058 men in a cross-sectional study and from 560 men with normal glucose tolerance (NGT) in a longitudinal study.

Key messages

- Low lung volume was significantly associated with the incidence of prediabetes or diabetes mellitus (DM) in both cross-sectional and longitudinal studies.
- Low lung volume is an independent risk factor for a particular type of prediabetes, impaired glucose tolerance rather than impaired fasting glucose. Our results suggested that prediabetes is not associated with the early stage of COPD, although there are published evidences for an association between COPD and DM.

Strengths and limitations of this study

- This is the first study that prospectively examined the incidence of newly diagnosed prediabetes among subjects with NGT at baseline. There are several limitations including that the subjects were limited to Japanese men and our occupational cohort may possibly be healthier than the general population.

function and diabetes mellitus (DM). Population-based studies have demonstrated associations between both obstructive and restrictive lung impairment and insulin resistance or DM.^{1–9} A representative obstructive lung disease, chronic obstructive pulmonary disease (COPD), is now well known to be associated with a variety of comorbidities, including DM.^{10–13} However, an accelerated decline of lung function has been observed in patients with DM.¹⁴ The incidence rates of COPD, asthma, lung fibrosis and pneumonia

are greater in patients with DM than in those without DM.¹⁵ The incidence of death from COPD is also increased in DM.¹⁶

The metabolic stage between normal glucose homeostasis and DM is called prediabetes, which the WHO divides into impaired glucose tolerance (IGT) and increased fasting glucose (IFG).¹⁷ Both IFG and IGT are the established risk factors for DM.¹⁸ The Diabetes Prevention Program Research Group¹⁵ found that about 30% of subjects with prediabetes developed DM during 3–5 years of follow-up. IFG and IGT are also risk factors for cardiovascular disease (CVD), relationships that are not confounded by the development of DM.^{19–20} Subjects with prediabetes also have higher incidence rates of microvascular complications, including neuropathy, retinopathy and nephropathy, than do those with normal glucose tolerance (NGT).^{21–22}

We reported previously that smokers with airflow limitation had subclinical atherosclerosis as evidenced by carotid intima-media thickness (CIMT).¹² Although we excluded subjects with DM, the prediabetic state may influence the association, since prediabetes per se was accompanied by a modest but significant increase in the risk for developing CVD, as described above. However, there is no information regarding the association between lung function and prediabetes. Therefore, we explored the incidence of newly diagnosed prediabetes among selected subjects with NGT to further elucidate the nature of the relationship between lung function and the development of DM.

METHODS

Subjects

The subjects were recruited from 1218 men who attended the Nippon Telegraph and Telephone West Corporation Chugoku Health Administration Center for general health checkups between April 1999 and March 2006. One hundred and sixty subjects were excluded, because they did not meet the following inclusion criteria: (1) between 40 and 59 years of age at the first examination, and able to perform both a 75 g oral glucose tolerance test (OGTT) and adequate spirometric measurements (146 subjects excluded); (2) no known respiratory disease (14 excluded). Data from the remaining 1058 subjects were used for a baseline cross-sectional analysis. For the longitudinal study, subjects were restricted to those who had NGT (365 excluded), and could be followed up for more than 20 months (133 excluded). The remaining 560 subjects were included. Among these subjects, 77 were receiving medication for hypertension, 43 for dyslipidaemia and 11 for hyperuricaemia. The distributions of these subjects among the quartiles of percent predicted value of %FVC and percent value of 1 s/FVC (FEV₁/FVC ratio) were not significantly different.

The study was approved by the Ethical Committee of Kochi University.

75 g oral glucose tolerance test

DM and prediabetes were diagnosed according to the 2003 criteria of the WHO.¹⁷ Subjects with prediabetes were classified into two categories: isolated IFG and IGT. Isolated IFG was defined as a fasting plasma glucose level of 6.1–6.9 mmol/l and a 2 h postload plasma glucose level of <7.8 mmol/l; and IGT was defined by a fasting plasma glucose level of <7.0 mmol/l and a 2 h postload plasma glucose level of 7.8–11.1 mmol/l. Blood samples were collected after a 10 h fast, and then 2 h after a 75 g oral glucose load.

Fasting insulin was measured by an enzyme immunoassay (Dainabot, Tokyo, Japan) with an intra-assay coefficient of variation of 3.1–4.4%. The homeostasis model assessment (HOMA) formula, (fasting insulin (mU/l)×fasting glucose (mmol/l))/22.5, was used to calculate the insulin resistance score.

Pulmonary function test

Pulmonary function was measured using a spirometer (Chest HI-801; Chest Co., Tokyo, Japan) by an experienced technician according to the recommendations of the American Thoracic Society.²³ The Japanese reference values were used.²⁴

Statistical analysis

Statistical analysis was carried out using SPSS, V.18.0 (SPSS Japan Inc, Tokyo, Japan). Statistical comparisons of the baseline characteristics of each group were performed using either the χ -square test or one-way analysis of variance (ANOVA). Comparisons among the groups were performed by using post-hoc Tukey test. In the cross-sectional study, logistic regression models were used to estimate the relevant ORs. In the longitudinal study, the HR of each covariate for the risk of development of prediabetes with 95% CI was calculated using the Cox hazard model. Tests for a linear trend across increasing categories of spirometric indices were conducted by treating the categories as continuous variables in a model. In all analyses, $p < 0.05$ was taken to indicate statistical significance.

RESULTS

Baseline analysis

At baseline, our study population (n=1058) consisted of 693 normal subjects, 93 with isolated IFG, 167 with IGT and 105 with DM. To examine the relationship between lung function parameters and impaired glucose metabolism, the subjects were divided into quartiles according to baseline %FVC and the FEV₁/FVC ratio. Some parameters, including age, body mass index (BMI), systolic blood pressure and total cholesterol, differed significantly among the quartiles (table 1). After adjustment for these parameters, impaired glucose metabolism was significantly associated with %FVC ($p < 0.001$), but not with the FEV₁/FVC ratio ($p = 0.80$). Specifically, IGT ($p = 0.04$) and DM ($p = 0.008$), but not isolated IFG ($p = 0.28$), were associated with %FVC (table 2).

Table 1 Baseline characteristics of subjects with NGT, isolated IFG, IGT and DM in the cross-sectional study

	NGT	Isolated IFG	IGT	DM	p Value
Number of subjects	693	93	167	105	
Current smokers (%)	48	42	45	50	0.54
Age (years)	49.5±5.5	50.9±5.3*	51.1±5.3**	52.2±4.7***	<0.001
Height (cm)	169.9±5.7	168.8±5.8	169.1±6.0	168.4±5.0*	0.03
BMI (kg/m ²)	23.1±2.5	23.9±3.1**	24.6±2.8***	24.8±3.2***	<0.001
Systolic BP (mm Hg)	126.4±16.3	135.1±16.4***	135.9±18.2***	140.2±16.3***	<0.001
Pack-year smoking	30.5±15.6	38.0±22.6*	31.1±17.3	38.0±18.5**	0.002
FEV ₁ /FVC (%)	80.1±7.0	79.6±7.8	80.9±7.4	79.4±8.5	0.36
%FVC	97.9±14.2	96.5±12.9	92.0±13.3***	89.2±15.7***	<0.001
Fasting glucose (mmol/l)	5.3±0.4	6.3±0.2***	5.9±0.5***	8.1±1.6***	<0.001
120 min glucose (mmol/l)	5.7±1.0	6.5±0.8***	8.8±0.8***	12.4±4.0***	<0.001
HbA1c (%)	5.10±0.33	5.34±0.36***	5.37±0.41***	6.57±1.20***	<0.001
HOMA-R	1.08±0.56	1.91±2.23**	1.56±0.88***	2.33±1.41***	<0.001
C reactive protein (mg/l)	0.11±0.29	0.09±0.14	0.14±0.28	0.18±0.46	0.13
T-chol (mg/dl)	202.1±32.6	210.0±28.7*	209.5±36.3*	214.8±32.2***	<0.001

Values are numbers, percentages (%) or means ±SD.

*p<0.05.

**p<0.01.

***p<0.001 vs NGT.

BMI, body mass index; BP, blood pressure; CRP, C reactive protein; DM, diabetes mellitus; HbA1c, glycated haemoglobin; HOMA-R, homeostasis model assessment of insulin resistance; IFG, increased fasting glucose; IGT, impaired glucose tolerance; NGT, normal glucose tolerance; T-chol, total cholesterol.

Frequencies of newly diagnosed prediabetes in subjects with NGT

After the observation period (mean±SD: 28.4 ±6.1 months), there were 44 subjects with isolated IFG and 58 with IGT among those previously categorised

as NGT (n=560), but no subject developed DM. As shown in table 3, there were significant differences in several parameters at baseline, including height, BMI, systolic blood pressure and %FVC, but not in FEV₁/FVC ratio.

Table 2 ORs*(95% CI) of prediabetes and DM according to the quartiles of %FVC† or FEV₁%‡ in the cross-sectional study

	I	II	III	IV	p for trend
IFG					
%FVC	1.0	4.60 (1.29 to 16.39)	2.03 (0.53 to 7.79)	2.57 (0.69 to 9.60)	0.06
FEV ₁ /FVC	1.0	1.00 (0.32 to 3.12)	1.39 (0.49 to 3.93)	1.81 (0.67 to 4.90)	0.53
IGT					
%FVC	1.0	1.35 (0.57 to 3.19)	2.18 (1.02 to 4.05)	2.59 (1.17 to 5.69)	0.04
FEV ₁ /FVC	1.0	0.60 (0.35 to 1.15)	0.62 (0.37 to 1.16)	0.50 (0.30 to 1.02)	0.12
IFG or IGT					
%FVC	1.0	2.18 (1.08 to 4.42)	2.09 (1.04 to 4.18)	2.55 (1.28 to 5.09)	<0.001
FEV ₁ /FVC	1.0	0.56 (0.31 to 1.07)	0.63 (0.35 to 1.14)	0.65 (0.36 to 1.17)	0.29
DM					
%FVC	1.0	3.77 (1.29 to 11.03)	1.28 (0.41 to 3.99)	2.50 (0.87 to 7.16)	0.02
FEV ₁ /FVC	1.0	2.08 (0.72 to 5.99)	3.05 (1.12 to 8.31)	2.13 (0.76 to 6.00)	0.18
IFG or IGT, or DM					
%FVC	1.0	3.32 (1.71 to 6.42)	2.04 (1.06 to 3.94)	3.33 (1.74 to 6.38)	<0.001
FEV ₁ /FVC	1.0	0.74 (0.40 to 1.35)	0.98 (0.56 to 1.75)	0.84 (0.48 to 1.49)	0.70

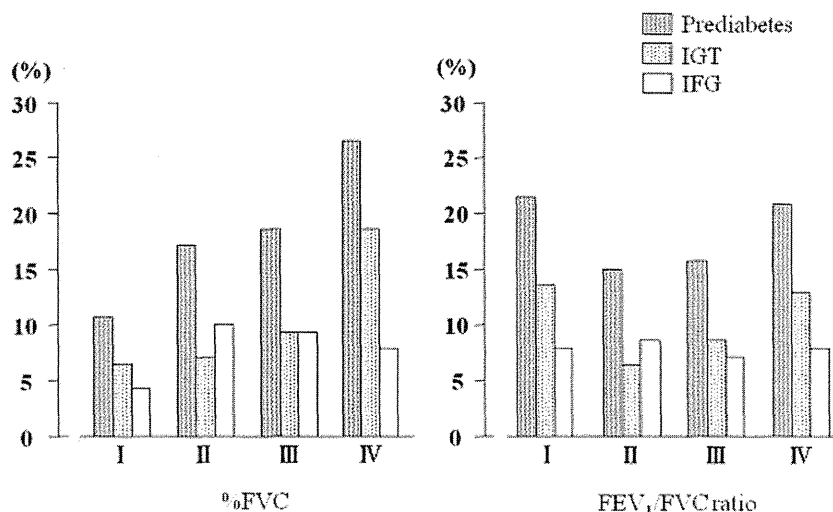
*OR was adjusted for age, BMI, pack-year smoking, systolic BP and T-chol.

†%FVC quartile: I (highest group) (≥104.2%), II (96.0%≤%FVC<104.2%), III (86.4%≤%FVC<96.0%), IV (lowest group) (%FVC<86.4%).

‡FEV₁/FVC quartile: I (highest group) (≥85.0), II (81.1%≤FEV₁/FVC<85.0%), III (76.5%≤FEV₁/FVC<81.1%), IV (lowest group) (FEV₁/FVC<76.5%).

BMI, body mass index; BP, blood pressure; DM, diabetes mellitus; IFG, impaired fasting glucose; IFG, increased fasting glucose; IGT, impaired glucose tolerance; T-chol, total cholesterol.

Figure 1 Incidences of newly diagnosed prediabetes, isolated IFG and impaired glucose tolerance (IGT) according to quartiles of % FVC and the FEV₁/FVC ratio. The incidence of prediabetes was significantly associated with %FVC, but not with the FEV₁/FVC ratio ($p=0.01$). Among subjects with prediabetes, lower %FVC was significantly associated with a higher incidence of IGT ($p=0.04$), but not of IFG ($p=0.47$).



Lung function parameters were divided into quartiles according to baseline %FVC and the FEV₁/FVC ratios. Among the quartiles the parameters, including age, BMI and systolic blood pressure, were significantly different (data not shown). Both in the crude model and following adjustment by age, BMI, pack-year smoking and systolic blood pressure, the development of prediabetes occurred significantly more frequently in the lowest quartile of % FVC, but not in that of the FEV₁/FVC ratio (table 4). Among prediabetes, IGT, but not isolated IFG, was significantly associated with %FVC, as in the baseline cross-sectional analysis (table 4; figure 1).

DISCUSSION

In the baseline cross-sectional study, we found that a low %FVC, but not a low FEV₁/FVC ratio, was significantly

associated with increased prevalences of prediabetes and DM. As lung function might be impaired by DM, a causal effect of lung function on DM could not be established by these data. Therefore, we also explored prospectively the effect of lung function on the development of newly diagnosed prediabetes in the population with normal glucose metabolism, as evidenced by the results of an OGTT. We found that reduced lung volume (%FVC), but not airflow limitation (FEV₁/FVC ratio), was significantly associated with the future development of prediabetes.

This study demonstrated that IGT, but not IFG, was closely associated with lower lung volume in both cross-sectional and longitudinal settings. Our finding was supported by previous studies conducted in an Asian population with relatively low BMI but high smoking

Table 3 Baseline characteristics of subjects who remained NGT, developed isolated IFG and IGT in the longitudinal study.

	NGT	Isolated IFG	IGT	p Value
Number of subjects	458	44	58	
Current smokers (%)	48	30*	50	0.05
Age (years)	49.3±5.7	50.2±4.4	50.5±4.9	0.14
Height (cm)	169.9±5.6	170.2±4.9	167.1±6.7**	0.01
BMI (kg/m ²)	23.0±2.5	23.8±2.3*	23.7±3.0*	0.04
Systolic BP (mm Hg)	125.4±16.7	130.5±16.9*	129.3±14.5	0.048
Pack-year smoking	29.9±15.6	31.1±12.1	30.1±18.5	0.97
FEV ₁ /FVC (%)	80.1±7.1	79.7±6.3	79.9±7.9	0.95
%FVC (%)	97.5±14.2	93.0±14.7*	90.0±16.0***	<0.001
Fasting glucose (mmol/l)	5.3±0.4	5.6±0.2***	5.5±0.3**	<0.001
120 min glucose (mmol/l)	5.6±0.9	6.0±1.2	6.4±0.9***	<0.001
HbA1c (%)	5.07±0.33	5.31±0.37***	5.19±0.30*	<0.001
HOMA-R	1.04±0.53	1.19±0.61	1.31±0.64**	0.001
C reactive protein (mg/l)	0.10±0.23	0.18±0.42	0.16±0.30	0.26
T-chol (mg/dl)	201.4±34.5	205.3±27.1	212.5±28.6*	0.05
Duration (month)	28.6±6.2	28.5±5.1	27.6±5.6	0.13

Values are number, percentage (%) or mean±SD.

* $p < 0.05$.

** $p < 0.01$.

*** $p < 0.001$ vs NGT.

BMI, body mass index; BP, blood pressure; CRP, C reactive protein; HOMA-R, homeostasis model assessment of insulin resistance; IFG, increased fasting glucose; IGT, impaired glucose tolerance; NGT, normal glucose tolerance; T-chol, total cholesterol.

Table 4 HRs (95% CI) for development of isolated IFG or IGT according to the quartiles of %FVC* or FEV₁%†

	I	II	III	IV	p for trend
IFG					
%FVC					
Model 1	1.0	0.85 (0.38 to 1.92)	0.81 (0.36 to 1.79)	1.96 (0.71 to 5.26)	0.31
Model 2	1.0	1.07 (0.48 to 2.39)	1.35 (0.60 to 3.03)	0.54 (0.20 to 1.49)	0.32
FEV₁/FVC					
Model 1	1.0	0.96 (0.42 to 2.17)	1.20 (0.51 to 2.86)	0.98 (0.43 to 2.27)	0.95
Model 2	1.0	0.99 (0.43 to 2.31)	0.84 (0.35 to 2.00)	1.04 (0.45 to 2.47)	0.96
IGT					
%FVC					
Model 1	1.0	1.96 (1.00 to 3.85)	2.63 (1.27 to 5.56)	3.03 (1.43 to 6.67)	0.006
Model 2	1.0	2.22 (1.02 to 3.88)	2.26 (1.07 to 4.78)	2.74 (1.26 to 5.98)	0.02
FEV₁/FVC					
Model 1	1.0	2.13 (0.96 to 4.76)	1.67 (0.81 to 3.45)	1.03 (0.54 to 1.96)	0.15
Model 2	1.0	2.09 (0.92 to 4.72)	1.69 (0.81 to 3.52)	1.11 (0.57 to 2.16)	0.10
IFG or IGT					
%FVC					
Model 1	1.0	2.13 (0.93 to 3.03)	1.85 (1.03 to 3.57)	2.63 (1.43 to 4.76)	0.01
Model 2	1.0	1.48 (0.89 to 2.44)	1.38 (0.82 to 2.34)	2.40 (1.30 to 4.44)	0.04
FEV₁/FVC					
Model 1	1.0	1.47 (0.84 to 2.56)	1.47 (0.85 to 2.56)	1.01 (0.61 to 1.69)	0.32
Model 2	1.0	1.47 (0.83 to 2.61)	1.47 (0.84 to 2.56)	1.09 (0.64 to 1.84)	0.21

*%FVC quartile; I (highest group) (≥ 106.0%), II (96.6% ≤ %FVC < 106.0%) III (88.1% ≤ %FVC < 96.6%), IV (lowest group) (%FVC < 88.1%).

†FEV₁/FVC quartile; I (highest group) (≥ 85.0%), II (80.9% ≤ FEV₁/FVC < 85.0%), III (76.0% ≤ FEV₁/FVC < 80.9%), IV (lowest group) (FEV₁/FVC < 76.0%).

IGT, impaired glucose tolerance; IFG, increased fasting glucose.

Model 1 denotes crude model and model 2, adjusted for age, BMI, pack-year smoking and systolic BP.

prevalence.^{8 9} In addition, such association between lower lung function and impaired glucose metabolism was also demonstrated in Western populations with higher BMI but lower smoking prevalence, and the association had been shown to be independent of smoking or obesity (refs. 1–6, for review ref. 7).

The mechanisms for the association are not clarified at present. It has been suggested that IGT is caused mainly by insulin resistance in the muscle, and IFG mainly by insulin resistance in the liver.²⁵ Reduced lung volume is associated with reduced maximum oxygen uptake, which may lead to poorer physical fitness and physical activity, and thus result in insulin resistance and DM.^{26–28} This may explain why IGT is more closely associated with lung volume. Furthermore, poorer lung function in adulthood may be due to low birth weight or early-life malnutrition,^{29 30} both of which have been reported to be associated with the development of diabetes.³¹ Malnutrition as a neonate may be an important early cause of cardiac and metabolic disorders in adulthood as a consequence of fetal programming.^{32 33}

This study had several limitations. The study population was limited to men, owing to the fact that sufficient

female subjects were not available at the institute. The occupational cohort used in this study may not be representative of Japanese men in general. For example, the prevalence rates of hypertension and hyperlipidaemia in this cohort were 13% and 7%, respectively (data not shown). The National Health and Nutrition Examination Survey in Japan showed prevalence rate of these in general Japanese men aged 40–60 years, in general, were around 30% and 35%, respectively, suggesting that our occupational cohort may be healthier. Subjects taking medications, including simvastatin, which have been shown to lower the risk of impaired glucose metabolism were not excluded, although the distributions of %FVC and the FEV₁/FVC ratio in those taking drugs for hypertension, dyslipidaemia and hyperuricaemia were not significantly different from those of subjects not on such medication.

In conclusion, this study provides evidence for a prospective relationship between lung volume and the incidence of newly diagnosed prediabetes among subjects with normal glucose metabolism at baseline. Among subjects with prediabetes, the study also suggests that lung volume may be a risk factor for the development of IGT, which is mainly caused by insulin resistance in the

muscle, but not IFG, which is caused mainly by insulin resistance in the liver. Although there is published evidence for an association between COPD and DM, our results suggest that prediabetes is not associated with at least the early stage of COPD.

Acknowledgements The authors would like to thank the staff of Nippon Telegraph and Telephone West Corporation Chugoku Health Administration Center.

Contributors TY contributed to the collection of data, analysis and interpretation of data, and writing of the draft. AY contributed to the study design, analysis and interpretation of data, editing of the draft and acquisition of funding. YK and SM contributed to the collection of data and analysis, YH, NH and KY contributed to the collection and interpretation of data, and editing the draft. NK contributed to the analysis and interpretation of data, and editing of the draft. All authors read and approved the final manuscript.

Funding This work was supported in part by a grant-in-aid for scientific research from the Ministry of Education, Culture, Sports, Science and Technology of Japan (No. 23390222 and 24659405), and a grant to the Respiratory Failure Research Group from the Ministry of Health, Labor and Welfare, Japan.

Competing interests None.

Patient consent Obtained.

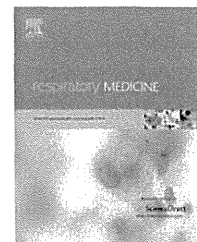
Ethics approval The Ethical Committee of Kochi University.

Provenance and peer review Not commissioned; externally peer reviewed.

Data sharing statement No additional data are available.

REFERENCES

- Engström G, Janzon L. Risk of developing diabetes is inversely related to lung function: a population-based cohort study. *Diabet Med* 2002;19:167–70.
- Ford ES, Mannino DM; National Health and Nutrition Examination Survey Epidemiologic Follow-up Study. Prospective association between lung function and the incidence of diabetes: findings from the National Health and Nutrition Examination Survey Epidemiologic Follow-up Study. *Diabetes Care* 2004;27:2966–70.
- Lawlor DA, Ebrahim S, Smith GD. Associations of measures of lung function with insulin resistance and type 2 diabetes: findings from the British Women's Heart and Health Study. *Diabetologia* 2004;47:195–203.
- Yeh HC, Punjabi NM, Wang NY, et al. Cross-sectional and prospective study of lung function in adults with type 2 diabetes: the atherosclerosis risk in communities (ARIC) study. *Diabetes Care* 2008;31:741–6.
- Lee HM, Le H, Lee BT, et al. Forced vital capacity paired with Framingham Risk Score for prediction of all-cause mortality. *Eur Respir J* 2010;36:1002–6.
- Hickson DA, Burchfiel CM, Liu J, et al. Diabetes, impaired glucose tolerance, and metabolic biomarkers in individuals with normal glucose tolerance are inversely associated with lung function: the Jackson Heart Study. *Lung* 2011;189:311–21.
- Klein OL, Krishnan JA, Glick S, et al. Systematic review of the association between lung function and type 2 diabetes mellitus. *Diabet Med* 2010;27:977–87.
- Heianza Y, Arase Y, Tsuji H, et al. Low lung function and risk of type 2 diabetes in Japanese men: the Toranomon Hospital Health Management Center Study 9 (TOPICS 9). *Mayo Clin Proc* 2012;87:853–61.
- Kwon CH, Rhee EJ, Song JU, et al. Reduced lung function is independently associated with increased risk of type 2 diabetes in Korean men. *Cardiovasc Diabetol* 2012;11:38.
- Sinden NJ, Stockley RA. Systemic inflammation and comorbidity in COPD: a result of 'overspill' of inflammatory mediators from the lungs? Review of the evidence. *Thorax* 2010;65:930–6.
- Mannino DM, Thorn D, Swensen A, et al. Prevalence and outcome of diabetes, hypertension and cardiovascular disease in COPD. *Eur Respir J* 2008;32:962–9.
- Iwamoto H, Yokoyama A, Kitahara Y, et al. Airflow limitation in smokers is associated with subclinical atherosclerosis. *Am J Respir Crit Care Med* 2009;179:35–40.
- Feary JR, Rodrigues LC, Smith CJ, et al. Prevalence of major comorbidities in subjects with COPD and incidence of myocardial infarction and stroke: a comprehensive analysis using data from primary care. *Thorax* 2010;65:956–62.
- Davis WA, Knudman M, Kendall P, et al. Glycemic exposure is associated with reduced pulmonary function in type 2 diabetes: the Fremantle Diabetes Study. *Diabetes Care* 2004;27:752–7.
- Ehrlich SF, Quesenberry CP Jr, Van Den Eeden SK, et al. Patients diagnosed with diabetes are at increased risk for asthma, chronic obstructive pulmonary disease, pulmonary fibrosis, and pneumonia but not lung cancer. *Diabetes Care* 2010;33:55–60.
- Seshasai SR, Kaptoge S, Thompson A, et al. Diabetes mellitus, fasting glucose, and risk of cause-specific death. *N Engl J Med* 2011;364:829–41.
- World Health Organization. Definition and diagnosis of diabetes mellitus and intermediate hyperglycemia: report of a WHO/IDF consultation. Geneva: World Health Organization, 2006.
- Knowler WC, Barrett-Connor E, Fowler SE, et al. Reduction in the incidence of type 2 diabetes with lifestyle intervention or metformin. *N Engl J Med* 2002;346:393–402.
- Unwin N, Shaw J, Zimmet P, et al. Impaired glucose tolerance and impaired fasting glycaemia: the current status on definition and intervention. *Diabetes Med* 2002;19:708–23.
- Qiao Q, Jousilahti P, Eriksson J, et al. Predictive properties of impaired glucose tolerance for cardiovascular risk are not explained by the development of overt diabetes during follow-up. *Diabetes Care* 2003;26:2910–14.
- Gabir MM, Hanson RL, Dabelea D, et al. Plasma glucose and prediction of microvascular disease and mortality: evaluation of 1997 American Diabetes Association and 1999 World Health Organization criteria for diagnosis of diabetes. *Diabetes Care* 2000;23:1113–18.
- Singleton JR, Smith AG, Bromberg MB. Increased prevalence of impaired glucose tolerance in patients with painful sensory neuropathy. *Diabetes Care* 2001;24:1448–53.
- American Thoracic Society. Standardization of spirometry, 1994 update. *Am J Respir Crit Care Med* 1995;152:1107–36.
- Committee report of pulmonary physiology in Japan Respiratory Society. Reference values for spirogram and arterial blood gas analysis in Japanese. (In Japanese.) *Nihon Kokyoku Gakkai Zasshi* 2001;39:1S–17S.
- Abdul-Ghani MA, Jenkinson CP, Richardson DK, et al. Insulin secretion and action in subjects with impaired fasting glucose and impaired glucose tolerance: results from the Veterans Administration Genetic Epidemiology Study. *Diabetes* 2006;55:1430–5.
- Eriksson KF, Lindgärde F. Poor physical fitness, and impaired early insulin response but late hyperinsulinaemia, as predicts of NIDDM in middle-aged Swedish men. *Diabetologia* 1996;39:573–9.
- Burney PG, Hooper R. Forced vital capacity, airway obstruction and survival in a general population sample from the USA. *Thorax* 2011;66:49–54.
- Guerra S, Sherrill DL, Venker C, et al. Morbidity and mortality associated with the restrictive spirometric pattern: a longitudinal study. *Thorax* 2011;65:499–504.
- Orfel L, Strachan DP, Rudnicka AR, et al. Early influences on adult lung function in two national British cohorts. *Arch Dis Child* 2008;93:570–4.
- Sebert S, Sharkey D, Budge H, et al. The early programming of metabolic health: is epigenetic setting the missing link? *Am J Clin Nutr* 2011;94:1953S–8S.
- Whincup PH, Kaye SJ, Owen CG, et al. Birth weight and risk of type 2 diabetes: a systematic review. *JAMA* 2008;300:2886–97.
- Osmond C, Barker DJ. Fetal, infant, and childhood growth are predictors of coronary heart disease, diabetes, and hypertension in adult men and women. *Environ Health Perspect* 2000;108:545S–53S.
- Barker DJ. The developmental origins of adult disease. *J Am Coll Nutr* 2004;23:588S–95S.



Characteristics of inspiratory and expiratory reactance in interstitial lung disease



A. Sugiyama, N. Hattori*, Y. Haruta, I. Nakamura,
M. Nakagawa, S. Miyamoto, Y. Onari, H. Iwamoto,
N. Ishikawa, K. Fujitaka, H. Murai, N. Kohno

Department of Molecular and Internal Medicine, Institute of Biomedical & Health Sciences,
Hiroshima University, 1-2-3 Kasumi, Minami-ku, Hiroshima 734-8551, Japan

Received 4 July 2012; accepted 8 March 2013

Available online 10 April 2013

KEYWORDS

Forced oscillometry;
Impulse oscillation
system;
Interstitial lung
disease;
Reactance;
Within-breath change

Summary

Background: Forced oscillometry is a non-invasive method to measure respiratory resistance and reactance. In this study, we investigated the characteristics of measurements obtained with an impulse oscillation system (IOS) for patients with interstitial lung disease (ILD).

Method: IOS and spirometry were performed in 64 ILD patients, 54 asthma patients, 49 chronic obstructive pulmonary disease (COPD) patients, and 29 controls. Respiratory resistance and reactance were assessed as measurements averaged over several tidal breaths (whole-breath analysis) and as measurements separately averaged during inspiration and expiration (inspiratory–expiratory analysis).

Results: Whole-breath IOS analyses for ILD patients showed increased resistance at 5 Hz and decreased reactance at 5 Hz (X_5) compared with controls, although these features were also found in asthma and COPD patients. Inspiratory–expiratory analysis demonstrated that the changes in X_5 and reactance area (AX) between inspiration and expiration (ΔX_5 and ΔAX , respectively) were significantly different from those in asthma patients, COPD patients, and controls. However, multiple linear regression analysis showed that the presence of ILD was independently associated with ΔX_5 , but not with ΔAX . Furthermore, ΔX_5 was inversely correlated with vital capacity and diffusing capacity of carbon monoxide in ILD patients.

Conclusions: Our results suggest that ΔX_5 is a characteristic feature of IOS measurements in ILD patients, which is clearly different from those in asthma and COPD patients. This within-breath X_5 change in ILD might be associated with its severity and physiological abnormality, although further studies are needed to investigate its cause.

© 2013 Elsevier Ltd. All rights reserved.

* Corresponding author. Tel.: +81 82 257 5196; fax: +81 82 255 7360.
E-mail address: nhattori@hiroshima-u.ac.jp (N. Hattori).

Introduction

Interstitial lung disease (ILD) is a group of lung diseases with diverse clinical and histopathological manifestations that share a common physiological abnormality of restrictive ventilation.¹ In patients with ILD, a static expiratory pressure–volume curve of the lung is generally shifted downward and rightward and spirometry results reveal reduced vital capacity.² However, reduced vital capacity may occur even in patients with obstructive lung diseases and in other situations, such as chest wall restriction, lung resection, inspiratory muscle weakness, or poor cooperation with spirometry. In addition, spirometry is sometimes difficult to perform with elderly, cognitively impaired patients, or patients with severe respiratory distress.³

Forced oscillometry is a non-invasive method to measure respiratory impedance and generally requires only passive patient cooperation. Two components of respiratory impedance can be evaluated by forced oscillometry: total respiratory resistance and reactance.⁴ Resistance at low frequency, 5 Hz (R5), indicates total airway resistance and resistance at high frequency, 20 Hz (R20), approximates central airway resistance. The difference between R5 and R20 (R5 – R20) is considered to be an index of the small airways.³ Reactance at 5 Hz (X5) is thought to be reciprocally related to compliance. The resonant frequency (Fres) is the intermediate frequency at which the total reactance is 0, and reactance area (AX) is the integrated low frequency respiratory reactance magnitude (area under the curve) between 5 Hz to Fres.⁵ X5, Fres, and AX have been proposed for detecting expiratory flow limitations.^{6–8}

Forced oscillometry has been used primarily for patients with obstructive lung diseases because it can sensitively detect increased airway resistance.⁴ Additionally, Dellaca et al. reported that reactance assessed separately during inspiration and expiration (inspiratory–expiratory analysis) using forced oscillometry can accurately detect expiratory flow limitation.⁶ Inspiratory–expiratory analysis is useful to differentiate chronic obstructive pulmonary disease (COPD) patients from asthmatics who have the same degree of airflow limitation evaluated by spirometry.⁷ However, characteristic findings of forced oscillometry performed for patients with restrictive lung diseases such as ILD have not been fully demonstrated^{9–13} and, to the best of our knowledge, there has been no published data regarding inspiratory–expiratory analysis using forced oscillometry in patients with ILD. To date, forced oscillometry has not been shown to be able to distinguish between restrictive and obstructive lung disease.^{9,10}

In the present study, in order to investigate the characteristics of data obtained by forced oscillometry performed for patients with ILD, we measured respiratory resistance and reactance at both inspiratory and expiratory phases using an impulse oscillation system (IOS) in control subjects and in patients with ILD, COPD, and asthma. We also evaluated the relationships between the IOS measurements and results from pulmonary function tests for patients with ILD.

Materials and methods

Subjects

This was a retrospective observational study for subjects who had spirometry tests and IOS measurements at the Hiroshima University Hospital (Hiroshima, Japan) between December 2007 and April 2011. We enrolled 64 patients with ILD (36 males; mean age 65.8 ± 0.9 years), 54 patients with asthma (13 males; mean age 52.1 ± 2.6 years), 49 patients with COPD (40 males; mean age 71.5 ± 1.4 years), and 29 control subjects (19 males; mean age 47.6 ± 2.5 years). All ILD patients were diagnosed in accordance with the clinical criteria established by the current ATS/ERS guidelines.¹ Patients with ILD whose forced expiratory volume in 1 s (FEV₁)/forced vital capacity (FVC) ratio was <70% and/or who had a history of asthma were excluded from this study. Three ILD patients whose FEV₁/FVC ratios were <70% were excluded. All 3 of these patients were heavy smokers with rheumatoid arthritis and their CT results demonstrated the presence of apparent emphysema.

Clinical or histopathological diagnoses in the 64 enrolled patients with ILD were: idiopathic pulmonary fibrosis (IPF) in 26, nonspecific interstitial pneumonia (NSIP) in 17, chronic hypersensitivity pneumonia (CHP) in 7, collagen-vascular disease associated interstitial pneumonia (CVD-IP) in 13, and desquamative interstitial pneumonia in one patient. Regarding CVD-IP, cases whose chest CT results showed a usual interstitial pneumonia (UIP) or NSIP pattern were selected. Ten patients were treated with corticosteroids alone, two patients were treated with corticosteroids plus immunosuppressive agents, and one patient was treated with an immunosuppressive agent alone. Asthma diagnosis was made based on clinical history plus historical evidence of reversible airway obstruction. To avoid the possible complication of COPD, only asthmatic patients who never smoked were enrolled. For the 54 enrolled patients, asthma severity based on the Global Initiative for Asthma (GINA) criteria¹⁴ was step 1 for 7 patients (13.0%), step 2 for 11 patients (20.4%), step 3 for 12 patients (22.2%), step 4 for 18 patients (33.3%), and step 5 for 6 patients (11.1%). All enrolled asthma patients had not suffered from exacerbations during the previous month. Among the 54 patients with asthma, inhaled corticosteroids were used by 44 patients, long acting β_2 -agonists were used by 22 patients, anti-leukotriene receptor antagonists were used by 14 patients, and oral theophylline was used by 11 patients. A COPD diagnosis was based on the Global Initiative for Obstructive Lung Disease (GOLD) criteria.¹⁵ COPD severity according to the GOLD criteria was stage 1 (mild) for 6 patients, stage 2 (moderate) for 24, stage 3 (severe) for 18, and stage 4 (very severe) for 1. Each enrolled COPD patient was clinically stable. Among the 49 COPD patients, a long acting anti-cholinergic agent was used by 20 patients, long acting β_2 -agonists were used by 19 patients, and inhaled corticosteroids were used by 13 patients. All of the control subjects were non-current smokers who had visited the Hiroshima University Hospital for medical health check-ups. Spirometric results for all control subjects were FEV₁/FVC ratio >70% and vital capacity (VC) >80% of predicted. None of the control subjects had evidence of pulmonary

disease based on their histories and physical examination results.

All subjects were informed of the possibility of being enrolled in a retrospective observational study when they had spirometry tests and IOS measurements, and all provided permission to use their de-identified data. The institutional review board approved this retrospective observational study and waived the requirement to obtain informed consent.

Forced oscillometry

In this study, we used IOS (Eric Jaeger, Germany) to assess respiratory impedance. IOS measurements were performed before spirometry. Impulses were applied for 30 s during tidal breathing in a sitting position. Subjects supported their cheeks with both hands to reduce upper airway shunting and wore nose clips to avoid air leaks. R5, R20, R5 – R20, X5, Fres, and AX were evaluated. We compared the data for R5, R20, R5 – R20, X5, Fres, and AX measured at inspiratory and expiratory phases. The results for each of these variables were determined using IOS software by separately averaging the measurements obtained during inspiration and expiration. Within-breath changes in X5 ($\Delta X5$), defined as expiratory X5 minus inspiratory X5, and in AX (ΔAX), defined as expiratory AX minus inspiratory AX, were compared among the four groups.

Pulmonary function tests

Spirometry and diffusion capacity for carbon monoxide (DLco) measurements were made by one specialist technician, as previously recommended.¹⁶ Predicted values for FEV₁, VC, and DLco were determined based on reference values.^{17,18} DLco was determined only for the patients with ILD using a single-breath technique. All DLco measurements were corrected to the standard haemoglobin value according to ERS/ATS standards.¹⁹

Statistical analysis

Results are expressed as the means \pm standard errors of the means (SEMs). A value of $p < 0.05$ was considered to indicate a significant difference. The Mann–Whitney test was

applied to examine differences between groups. Multiple linear regression analysis was used to assess the relative contributions of age, sex, height, weight, body mass index (BMI), and smoking status (pack-years) on $\Delta X5$ and ΔAX in the study groups (control, asthma, COPD, and ILD). Pearson correlation analysis was used to assess associations between $\Delta X5$ and %VC or %DLco in ILD patients. A Kruskal–Wallis test was used to compare the results for each variable among ILD subgroups. Statistical analyses were performed using the JMP software suite (SAS Institute).

Results

The subjects enrolled in the study were classified into control, asthma, COPD, and ILD groups. The subjects' characteristics are summarized in Table 1. Subjects in the COPD group were the oldest and had the highest pack-year smoking history among the four groups. The ILD group showed the lowest VC and the COPD group had the lowest FEV₁. The characteristics of the ILD subgroups (IPF, NSIP, CHP, and CVD-IP) are also summarized in Supplemental Table 1.

The whole-breath IOS results for the four groups are shown in Table 2. The whole-breath IOS results for ILD subgroups are also shown in Supplemental Table 2. R5 values in the control group (0.26 ± 0.01 kPa/L/s) were significantly lower than those in the asthma group (0.38 ± 0.02 kPa/L/s; $p < 0.0001$), the COPD group (0.42 ± 0.03 kPa/L/s; $p < 0.0001$), and the ILD group (0.31 ± 0.01 kPa/L/s; $p < 0.05$). However, R5 in the asthma or the COPD group was shown to be significantly higher as compared with that in the ILD group. While R20 was significantly higher in the asthma group than in the control group, there was no difference in R20 between the patients with ILD and the control subjects. R5 – R20 values were the highest in the COPD group among the four groups and were significantly higher in the asthma or the ILD group than in the control subjects.

Regarding X5, as compared with the control subjects (-0.10 ± 0.01 kPa/L/s), X5 values were significantly more negative in the patients with asthma (-0.16 ± 0.01 kPa/L/s; $p < 0.01$), COPD (-0.20 ± 0.02 kPa/L/s; $p < 0.0001$), and ILD (-0.16 ± 0.01 kPa/L/s; $p < 0.0001$). Fres and AX values in the asthma, COPD, and ILD groups were significantly higher than

Table 1 Study subjects' characteristics.

	Control (n Z 29)	Asthma (n Z 54)	COPD (n Z 49)	ILD (n Z 64)
Male/Female	19/10	13/41*	40/9 [†]	36/28 ^{†#}
Age (years)	47.6 \pm 2.5	52.1 \pm 2.6	71.5 \pm 1.4* [†]	65.8 \pm 0.9* ^{†#}
Body height (m)	1.65 \pm 0.02	1.55 \pm 0.01*	1.61 \pm 0.01* [†]	1.58 \pm 0.01* [†]
BMI (kg/m ²)	23.3 \pm 0.4	23.0 \pm 0.6	21.8 \pm 0.4*	23.1 \pm 0.5
Smoking history Current/Ex/Never	0/10/19	0/0/54	9/38/2	6/35/23
Pack-years	3.0 \pm 1.1	0*	53.9 \pm 3.8* [†]	27.5 \pm 3.5* ^{†#}
VC (% predicted)	105.1 \pm 1.8	95.1 \pm 2.6*	87.6 \pm 2.9* [†]	76.1 \pm 2.6* ^{†#}
FEV ₁ (% predicted)	103.2 \pm 2.1	86.1 \pm 2.8*	58.5 \pm 2.6* [†]	79.6 \pm 2.4* ^{†#}

BMI Z body mass index; COPD Z chronic obstructive pulmonary disease; ILD Z interstitial lung disease; VC Z vital capacity; FEV₁ Z forced expiratory volume in 1 s. Results are means \pm SEMs. p -Values are not significant unless indicated. * $p < 0.05$: vs. control group. [†] $p < 0.05$: vs. asthma group. [#] $p < 0.05$: vs. COPD group.

Table 2 Whole-breath IOS results.

	Control (n Z 29)	Asthma (n Z 54)	COPD (n Z 49)	ILD (n Z 64)
R5 (kPa/l/s)	0.26 ± 0.01	0.38 ± 0.02*	0.42 ± 0.03*	0.31 ± 0.01*†#
R20 (kPa/l/s)	0.24 ± 0.01	0.32 ± 0.01*	0.28 ± 0.01†	0.24 ± 0.01†
R5 – R20 (kPa/l/s)	0.02 ± 0.01	0.07 ± 0.01*	0.13 ± 0.02*†	0.07 ± 0.01*#
X5 (Pa/l/s)	-0.10 ± 0.01	-0.16 ± 0.01*	-0.20 ± 0.02*	-0.16 ± 0.01*
Fres (Hz)	10.57 ± 0.57	14.82 ± 0.71*	20.76 ± 0.98*†	15.74 ± 0.51*#
AX (kPa/l/s Hz)	0.28 ± 0.02	0.79 ± 0.13*	1.56 ± 0.22*†	0.77 ± 0.01*#

COPD Z chronic obstructive pulmonary disease; ILD Z interstitial lung disease; R5 Z resistance at 5 Hz; R20 Z resistance at 20 Hz; X5 Z reactance at 5 Hz; Fres Z resonant frequency; AX Z reactance area. Results are means ± SEMs. *p*-values are not significant unless indicated. **p* < 0.05: vs. control group. †*p* < 0.05: vs. asthma group. #*p* < 0.05: vs. COPD group.

those for the control subjects. Next, we separately calculated the average values for R5, R20, R5 – R20, X5, Fres, and AX during expiration and inspiration; these within-breath IOS measurements are shown in Table 3. The within-breath IOS results for subgroups of ILD (IPF, NSIP, CHP, and CVD-IP) are also shown in Supplemental Table 3. As shown in Fig. 1A, expiratory R5 was significantly higher than inspiratory R5 in all groups. Similarly, expiratory R20 was higher than inspiratory R20 in all groups but a statistically significant difference was not observed in the patients with COPD (Fig. 1B).

Interestingly, expiratory R5 – R20 was significantly higher than inspiratory R5 – R20 in the COPD group, whereas there were no significant differences in R5 – R20 between expiration and inspiration in the asthma group, the ILD group, and the control subjects. In contrast to the changes in R5 and R20 between expiration and inspiration, the changes in X5 between inspiration and expiration were found to vary among the four groups (Fig. 1C). In the

control subjects and the patients with asthma, there was no significant difference between expiratory X5 and inspiratory X5. In the patients with COPD, expiratory X5 (-0.23 ± 0.03 kPa/L/s) was more negative than inspiratory X5 (-0.16 ± 0.01 kPa/L/s) (*p* < 0.05). In the patients with ILD, however, expiratory X5 (-0.14 ± 0.013 kPa/L/s) was found to be significantly less negative than inspiratory X5 (-0.19 ± 0.01 kPa/L/s) (*p* < 0.0001).

In the ILD group, there was a trend for increased inspiratory AX (0.86 ± 0.08 kPa/L/s) compared to expiratory AX (0.74 ± 0.07 kPa/L/s), whereas Fres did not differ between inspiration (15.54 ± 0.47 kPa/L/s) and expiration (15.89 ± 0.57 kPa/L/s) (Table 3). Supporting the changes seen in X5 between expiration and inspiration among the four groups, ΔX5 in the ILD group (0.04 ± 0.01 kPa/L/s) was significantly higher than those in the other three groups, and ΔX5 in the COPD group (-0.08 ± 0.02 kPa/L/s) was significantly lower than those in the other three groups

Table 3 Inspiratory–expiratory IOS results.

	Control (n Z 29)	Asthma (n Z 54)	COPD (n Z 49)	ILD (n Z 64)
R5 (kPa/l/s)				
Expiratory	0.28 ± 0.02 [§]	0.41 ± 0.02* [§]	0.45 ± 0.03* [§]	0.32 ± 0.01 ^{†#§}
Inspiratory	0.23 ± 0.01	0.34 ± 0.02*	0.37 ± 0.02*	0.29 ± 0.01*†#
R20 (kPa/l/s)				
Expiratory	0.26 ± 0.02 [§]	0.33 ± 0.01* [§]	0.30 ± 0.01†	0.25 ± 0.01 ^{†#§}
Inspiratory	0.22 ± 0.01	0.29 ± 0.01*	0.26 ± 0.01*†	0.22 ± 0.01 ^{†#}
R5 – R20 (kPa/l/s)				
Expiratory	0.02 ± 0.01	0.08 ± 0.01*	0.16 ± 0.02*† [§]	0.07 ± 0.01*#
Inspiratory	0.01 ± 0.01	0.05 ± 0.01*	0.10 ± 0.01*†	0.07 ± 0.01*#
X5 (kPa/l/s)				
Expiratory	-0.10 ± 0.01	-0.16 ± 0.02*	-0.23 ± 0.03*† [§]	-0.14 ± 0.01*# [§]
Inspiratory	-0.11 ± 0.01	-0.16 ± 0.01*	-0.16 ± 0.01*	-0.19 ± 0.01*†#
ΔX5	0.02 ± 0.01	0.00 ± 0.01	-0.08 ± 0.02*†	0.04 ± 0.01*†#
Fres (Hz)				
Expiratory	10.70 ± 0.67	15.30 ± 0.82*	21.75 ± 1.02*† [§]	15.89 ± 0.57*#
Inspiratory	10.46 ± 0.49	13.80 ± 0.62*	19.04 ± 0.96*†	15.54 ± 0.47*†#
AX (kPa/l/s Hz)				
Expiratory	0.26 ± 0.05	0.88 ± 0.15*	1.87 ± 0.24*† [§]	0.74 ± 0.07*#
Inspiratory	0.28 ± 0.05	0.67 ± 0.10*	1.04 ± 0.12*†	0.86 ± 0.08*†
ΔAX	-0.02 ± 0.03	0.22 ± 0.08*	0.82 ± 0.18*†	-0.12 ± 0.06*†#

COPD Z chronic obstructive pulmonary disease; ILD Z interstitial lung disease; R5 Z resistance at 5 Hz; R20 Z resistance at 20 Hz; X5 Z reactance at 5 Hz; Fres Z resonant frequency; AX Z reactance area. Results are means ± SEMs. *p*-values are not significant unless indicated. **p* < 0.05: vs. control group. †*p* < 0.05: vs. asthma group. #*p* < 0.05: vs. COPD group. §*p* < 0.05: vs. inspiratory phase.

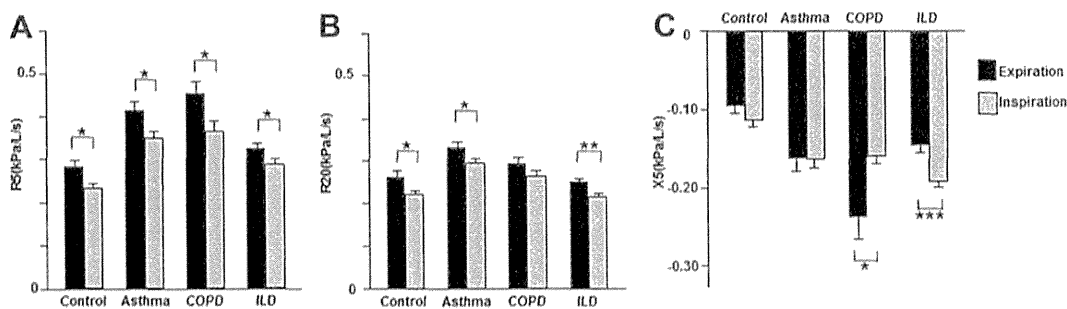


Figure 1 Comparisons of the mean values for resistance at 5 Hz (R5) (A), resistance at 20 Hz (R20) (B) and reactance at 5 Hz (X5) (C) during expiration and inspiration in the control ($n = 29$), asthma ($n = 54$), chronic obstructive pulmonary disease (COPD) ($n = 49$), and interstitial lung disease (ILD) ($n = 64$) groups. Error bars indicate standard errors of the mean. *: $p < 0.05$; **: $p < 0.01$; ***: $p < 0.0001$.

(Fig. 2A). In addition, ΔX values in the ILD group were significantly different from those in the other three groups (Fig. 2B). Among the asthma, COPD, ILD, and control groups, the variables of age, sex, height, weight, BMI, and smoking status (pack-years) were not completely matched; these differences might have affected the $\Delta X5$ and ΔX values. Therefore, we used multiple linear regression analysis to determine what variables were significantly associated with $\Delta X5$ or ΔX levels.

This analysis showed that $\Delta X5$ was independently associated with the presence of COPD ($b = -0.428$; $p < 0.0001$) or ILD ($b = 0.192$; $p = 0.037$), but was not associated with age, sex, height, weight, BMI, or smoking status (pack-year) (Table 4). The only significant variable associated with ΔX was the presence of COPD. An independent association between the presence of ILD and ΔX was not found. This result implied that $\Delta X5$ was a more characteristic feature of IOS measurements in ILD patients than was ΔX (Table 4). Based on these results, relationships between $\Delta X5$ and measurements of pulmonary function tests (%VC and %DLco) were analysed for ILD patients (Fig. 3). $\Delta X5$ was inversely correlated with %VC ($r = -0.43$; $p < 0.001$) and %DLco ($r = -0.57$; $p < 0.0001$).

Discussion

In the present study, the characteristics of IOS measurements made for patients with ILD were described in detail. To the best of our knowledge, this is the first report to compare IOS data between patients with restrictive and obstructive lung diseases. Whole-breath IOS analyses for ILD patients showed increased R5 and decreased X5 compared with controls, although these features were also found in the asthma and COPD groups. However, changes in IOS measurement results, particularly X5 and AX, between inspiration and expiration were characteristic features in asthma, COPD, and ILD. Inspiratory and expiratory X5 did not differ in the control subjects and the patients with asthma. The magnitudes of expiratory X5 were greater than those of inspiratory X5 in the patients with COPD, while this situation was found to be reversed in the patients with ILD. Similarly, the within-breath changes in AX were significantly lower in ILD patients than those in asthma or COPD patients; however, multiple linear regression analysis showed that the presence of ILD was not independently associated with ΔX . These results indicate that patients with ILD show completely different characteristics of

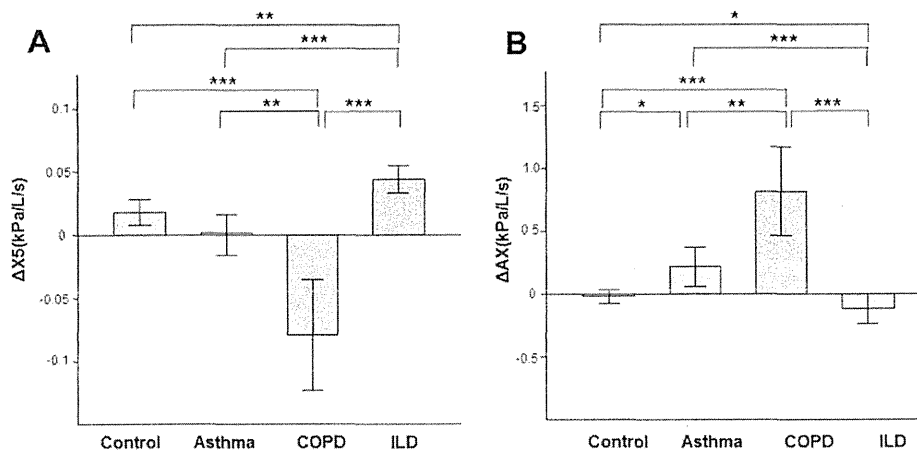


Figure 2 Comparison of the mean values for $\Delta X5$ (expiratory–inspiratory values of the reactance at 5 Hz) (A) and ΔAX (expiratory–inspiratory values of the reactance area) (B) in the control group ($n = 29$), patients with asthma ($n = 54$), patients with chronic obstructive pulmonary disease (COPD) ($n = 49$), and patients with interstitial lung disease (ILD) ($n = 64$). Error bars indicate standard errors of the mean. *: $p < 0.05$; **: $p < 0.01$; ***: $p < 0.0001$.

Table 4 Multiple linear regression analysis for $\Delta X5$ and ΔX .

Variables	$\Delta X5$		ΔX	
	Standardized coefficient (b)	p-Value	Standardized coefficient (b)	p-Value
Age	-0.006	0.946	-0.046	0.601
Sex	-0.055	0.548	0.045	0.634
Height	0.186	0.656	0.247	0.565
Weight	-0.267	0.687	-0.456	0.503
BMI	0.027	0.958	0.607	0.244
Smoking (pack-years)	0.074	0.417	-0.082	0.382
Control	0.072	0.350	-0.119	0.131
COPD	-0.428	<0.0001	0.449	<0.0001
ILD	0.192	0.037	-0.047	0.616

BMI Z body mass index; COPD Z chronic obstructive pulmonary disease; ILD Z interstitial lung disease. Sex: female Z 0, male Z 1; Control: no Z 0, yes Z 1; COPD: no Z 0, yes Z 1; ILD: no Z 0, yes Z 1. The presence of asthma was excluded from this multiple linear regression model.

within-breath changes in X5 as compared with asthma and COPD patients. In addition, a significant correlation between $\Delta X5$ and %VC or %DLco suggests that the within-breath change in X5 may be associated with a physiological abnormality in ILD.

The most interesting finding of this study was that the within-breath change in X5 was a distinguishable characteristic of ILD as compared with the change in asthma or COPD. As previously reported, there was no difference in X5 by whole-breath oscillometry between ILD and asthma or COPD.^{9,10} The magnitude of inspiratory X5 was shown to be greater than that of expiratory X5 in the patients with ILD. Consistent with the results of previous studies,^{3,6-8} the inspiratory and expiratory X5 did not differ in the asthma patients and the magnitude of inspiratory X5 was smaller than that of expiratory X5 in the patients with COPD. X5 is a numerically negative value thought to be related to the reciprocal of lung compliance.^{5,20} Therefore, its value becomes more negative when the peripheral lung tissue has reduced compliance or is compressed.^{20,21} Because the distensibility of peripheral lung tissue is decreased in patients with ILD,² compliance during inspiration is likely to be more reduced compared with that during expiration. This might be a reason why the magnitude of inspiratory X5

was greater than that of expiratory X5 in patients with ILD. Furthermore, the different patterns of within-breath changes in X5 among the patients with asthma, COPD, and ILD suggest that inspiratory–expiratory analysis using IOS might be useful not only for obstructive lung disease but also for ILD. Further investigations will be needed to identify the cause(s) of these differences of within-breath changes in X5.

Another interesting finding of this study was that $\Delta X5$ showed significant inverse correlations with VC and DLco in patients with ILD. Because reduced lung volume and diffusion capacity are associated with ILD disease severity and prognosis,^{22,23} our results may support the association between $\Delta X5$ and disease severity or physiological abnormality in ILD. The inverse correlation between $\Delta X5$ and VC may also suggest an association between increased $\Delta X5$ and reduced lung distensibility in ILD. In addition, the greater magnitude of $\Delta X5$ resulting from exaggerated inspiratory reactance may reflect an increased elastic recoil during inspiration in ILD.

For patients with ILD, whole-breath analyses of IOS demonstrated that R5 and R5 – R20 were increased, but that R20 was similar compared with those of the control subjects. Resistance represents the frictional components of the respiratory tract and is predominantly influenced by

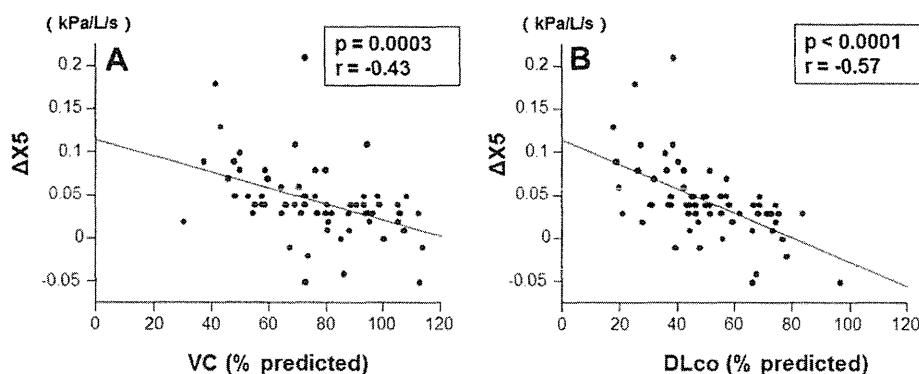


Figure 3 Relationship between $\Delta X5$ and VC% predicted (A) or DLco% predicted (B) in the patients with interstitial lung disease ($n = 64$). $\Delta X5$: within-breath change in reactance at 5 Hz (expiratory X5 minus inspiratory X5). VC: vital capacity. DLco: diffusing capacity of carbon monoxide.

the calibre of the central airways. Pressure oscillation at high frequency is severely dampened before reaching the peripheral airways, but it penetrates much further into the lung periphery at low frequency. Thus, R5 reflects total respiratory resistance, whereas R20 reflects central airway resistance. The difference between R5 and R20 (R5 – R20) is thought to be an index of the small airways.³ Based on these observations, R5, R20, and R5 – R20 results from ILD patients may suggest the presence of small airway disease²⁴; however, these results were not distinguishable from those for obstructive lung diseases.¹⁰ In addition, inspiratory–expiratory analyses of R5, R20, and R5 – R20 failed to discriminate ILD from obstructive lung diseases (Fig. 1A and B, Table 3). These results suggest that resistance measured using IOS cannot reveal the characteristics of ILD; however, inspiratory–expiratory analysis of reactance might show a distinctive pattern for ILD.

Although promising results were obtained, we are aware that this study has limitations. First, the number of the patients included in the study was relatively small. To verify the results, a larger sample size study is necessary. Secondly, for the data analysis, we used the raw values measured by IOS for various ages of subjects, since definitive predictive equations have not yet been established. Again, a large-scale study across a wider age range is needed to validate existing reference values.⁹

Conclusion

We have demonstrated that an increased magnitude of X5 during inspiration compared to X5 during expiration was a characteristic finding in inspiratory–expiratory analysis of IOS performed for patients with ILD. Significant inverse correlations between the magnitude of inspiratory–expiratory difference in X5 ($\Delta X5$) and VC or DLco were observed, and these data may suggest an association between $\Delta X5$ and severity and physiological abnormality in patients with ILD. $\Delta X5$ results showed clearly different patterns among patients with asthma, COPD, and ILD. Exaggerated inspiratory reactance in ILD may reflect reduced distensibility and increased elastic recoil of the lung during inspiration, although further studies are needed to investigate its cause.

Acknowledgement

The authors thank A. Matsubara for technical support of IOS measurement and spirometry.

Appendix A. Supplementary data

Supplementary data related to this article can be found online at <http://dx.doi.org/10.1016/j.rmed.2013.03.005>.

Conflict of interest

The authors declare that they have no competing interests.

References

1. American Thoracic Society/European Respiratory Society International Multidisciplinary Consensus Classification of the Idiopathic Interstitial Pneumonias. This joint statement of the American Thoracic Society (ATS), and the European Respiratory Society (ERS) was adopted by the ATS board of directors, June 2001 and by the ERS Executive Committee, June 2001. *Am J Respir Crit Care Med* 2002;165:277–304.
2. Thompson MJ, Colebatch HJ. Decreased pulmonary distensibility in fibrosing alveolitis and its relation to decreased lung volume. *Thorax* 1989;44:725–31.
3. Kubota M, Shirai G, Nakamori T, Kokubo K, Masuda N, Kobayashi H. Low frequency oscillometry parameters in COPD patients are less variable during inspiration than during expiration. *Respir Physiol Neurobiol* 2009;166:73–9.
4. Al-Mutairi SS, Sharma PN, Al-Alawi A, Al-Deen JS. Impulse oscillometry: an alternative modality to the conventional pulmonary function test to categorise obstructive pulmonary disorders. *Clin Exp Med* 2007;7:56–64.
5. MacLeod D, Birch M. Respiratory input impedance measurement: forced oscillation methods. *Med Biol Eng Comput* 2001;39:505–16.
6. Dellaca RL, Santus P, Aliverti A, Stevenson N, Centanni S, Macklem PT, Pedotti A, Calverley PM. Detection of expiratory flow limitation in COPD using the forced oscillation technique. *Eur Respir J* 2004;23:232–40.
7. Paredi P, Goldman M, Alamen A, Ausin P, Usmani OS, Pride NB, Barnes PJ. Comparison of inspiratory and expiratory resistance and reactance in patients with asthma and chronic obstructive pulmonary disease. *Thorax* 2010;65:263–7.
8. Kanda S, Fujimoto K, Komatsu Y, Yasuo M, Hanaoka M, Kubo K. Evaluation of respiratory impedance in asthma and COPD by an impulse oscillation system. *Intern Med* 2010;49:23–30.
9. Oostveen E, MacLeod D, Lorino H, Farre R, Hantos Z, Desager K, Marchal F. The forced oscillation technique in clinical practice: methodology, recommendations and future developments. *Eur Respir J* 2003;22:1026–41.
10. van Noord JA, Clement J, Cauberghs M, Mertens I, Van de Woestijne KP, Demedts M. Total respiratory resistance and reactance in patients with diffuse interstitial lung disease. *Eur Respir J* 1989;2:846–52.
11. Fisher AB, DuBois AB, Hyde RW. Evaluation of the forced oscillation technique for the determination of resistance to breathing. *J Clin Invest* 1968;47:2045–57.
12. Obol BJ. Tests of ventilatory function not requiring maximal subject effort. II. The measurement of total respiratory impedance. *Am Rev Respir Dis* 1968;97:868–79.
13. Muller E, Vogel J. Measurement and model-interpretation of new parameters of lung mechanics (author's transl). *Z Erkr Atmungsorgane* 1981;157:340–4.
14. GINA Report. *Global strategy for asthma management and prevention*. <http://www.ginasthma.org/>; 2010.
15. Global Initiative for Chronic Obstructive Lung Disease. *Global strategy for the diagnosis, management and prevention of chronic obstructive pulmonary disease*. <http://www.goldcopd.org/>; 2010.
16. Miller MR, Hankinson J, Brusasco V, Burgos F, Casaburi R, Coates A, Crapo R, Enright P, van der Grinten CP, Gustafsson P, et al. Standardisation of spirometry. *Eur Respir J* 2005;26:319–38.
17. Society TJR, editor. *Spirometry, flow-volume curve, diffusion capacity of the lung*. Tokyo: The Japanese Respiratory Society; 2004.
18. Nishida O, Kannabe M, Sewake N, Takano M, Kawane H, Kodomari Y, Arita K, Nasuno H, Nishimoto Y. Pulmonary function in healthy subjects and its prediction: 5. Pulmonary diffusing capacity in adults. *Jpn J Clin Pathol* 1976;24:941–7.

19. Macintyre N, Crapo RO, Viegi G, Johnson DC, van der Grinten CP, Brusasco V, Burgos F, Casaburi R, Coates A, Enright P, et al. Standardisation of the single-breath determination of carbon monoxide uptake in the lung. *Eur Respir J* 2005;**26**:720–35.
20. Kolsum U, Borrill Z, Roy K, Starkey C, Vestbo J, Houghton C, Singh D. Impulse oscillometry in COPD: identification of measurements related to airway obstruction, airway conductance and lung volumes. *Respir Med* 2009;**103**:136–43.
21. Williamson PA, Clearie K, Menzies D, Vaidyanathan S, Lipworth BJ. Assessment of small-airways disease using alveolar nitric oxide and impulse oscillometry in asthma and COPD. *Lung* 2011;**189**:121–9.
22. Egan JJ, Martinez FJ, Wells AU, Williams T. Lung function estimates in idiopathic pulmonary fibrosis. the potential for a simple classification. *Thorax* 2005;**60**:270–3.
23. Martinez FJ, Flaherty K. Pulmonary function testing in idiopathic interstitial pneumonias. *Proc Am Thorac Soc* 2006;**3**: 315–21.
24. Fulmer JD, Roberts WC. Small airways and interstitial pulmonary disease. *Chest* 1980;**77**:470–2.

SK-216, an Inhibitor of Plasminogen Activator Inhibitor-1, Limits Tumor Progression and Angiogenesis

Takeshi Masuda¹, Noboru Hattori², Tadashi Senoo², Shin Akita¹, Nobuhisa Ishikawa², Kazunori Fujitaka², Yoshinori Haruta², Hiroshi Murai², and Nobuoki Kohno²

Abstract

Plasminogen activator inhibitor-1 (PAI-1), which can be produced by host and tumor cells in the tumor microenvironment, is intimately involved in tumor progression. In the present study, to pursue the possibility that PAI-1 could be a therapeutic target in the management of malignancy, SK-216, a specific PAI-1 inhibitor, was orally administered to wild-type mice that were subcutaneously implanted or intravenously injected with either PAI-1-secreting Lewis lung carcinoma (LLC) or PAI-1-nonsecreting B16 melanoma cells. The systemic administration of SK-216 was found to reduce the size of subcutaneous tumors and the extent of metastases, regardless of PAI-1 secretion levels from the tumor cells. SK-216 also reduced the extent of angiogenesis in the tumors and inhibited VEGF-induced migration and tube formation by human umbilical vein endothelial cells *in vitro*. Then, to determine whether host or tumor PAI-1 was more crucial in tumor progression and angiogenesis, PAI-1-deficient or wild-type mice were subcutaneously implanted or intravenously injected with LLC or PAI-1 knockdown LLC cells. Tumor progression was shown to be controlled by the presence of host PAI-1 and not affected by the PAI-1 levels in the tumors. Similarly, host PAI-1 played a more crucial role in tumor angiogenesis than did tumor PAI-1. These observations suggest that regardless of the PAI-1 levels in the tumor, the systemic administration of SK-216 exerts an antitumor effect through its interaction with host PAI-1. This antitumor effect might be mediated by the antiangiogenic properties of SK-216. *Mol Cancer Ther*; 12(11); 2378–88. ©2013 AACR.

Introduction

The plasminogen activation system, represented by urokinase-type plasminogen activator (uPA), the cellular receptor for uPA (uPAR), and its specific inhibitor, the plasminogen activator inhibitor-1 (PAI-1), plays a crucial role in tumor growth, invasion, metastasis, and angiogenesis. The interaction between uPA and uPAR is believed to be a particularly efficient proteolytic system for endothelial and tumor cells to breakdown the extracellular matrix (ECM) during migration (1). In addition, through binding to uPA, uPAR transduces signals that promote cell migration and proliferation (2). Judging from these observations, PAI-1, a primary inhibitor of uPA, has long been considered a cancer inhibitor (3). However, recent evidence now shows an association between high expression of PAI-1 and poor prognosis in various types of tumors (4–

10). In addition, a large number of animal and/or *in vitro* studies have revealed the involvement of PAI-1 in tumor growth and metastasis through several possible mechanisms. Experiments using PAI-1-deficient (PAI-1^{-/-}) mice have shown the significance of host PAI-1 in regulating tumor angiogenesis (11–14). This process is thought to be mediated by the actions of PAI-1 on endothelial cells, thereby regulating plasmin-mediated proteolysis (15, 16), modulating migration (17, 18), and/or preventing apoptosis (19). PAI-1 is also known to be associated with cell motility. Binding of PAI-1 to the ECM protein vitronectin blocks the interaction between the integrins and the uPAR–uPA complex with vitronectin, thereby inhibiting adhesion and accelerating migration of cells (17, 18). Furthermore, recent studies have revealed that PAI-1 has a direct effect on pro-proliferative (20) and antiapoptotic signaling (21) in tumor cells. These observations clearly suggest an important role of PAI-1 in tumor progression.

In the tumor microenvironment, PAI-1 can be produced by host and tumor cells. There may be interactions between host and tumor PAI-1 and they likely differ in their relevance to tumor progression. However, whether host or tumor PAI-1 is more crucial to tumor progression is unknown. To date, deficiency of host PAI-1 has been clearly shown to reduce tumor progression through inhibiting tumor angiogenesis (11–14). In addition, recent studies have reported the inhibitory effects of reduced tumor PAI-1 levels on tumor progression (22, 23).

Authors' Affiliations: ¹Department of Molecular and Internal Medicine, Graduate School of Biomedical & Health Sciences, ²Institute of Biomedical and Health Sciences, Hiroshima University, Hiroshima, Japan

Note: Supplementary data for this article are available at Molecular Cancer Therapeutics Online (<http://mct.aacrjournals.org/>).

Corresponding Author: Noboru Hattori, Department of Molecular and Internal Medicine, Institute of Biomedical & Health Sciences, Hiroshima University, 1-2-3 Kasumi, Minami-ku, Hiroshima 734-8551, Japan. Phone: 81-822575196; Fax: 81-82257360; E-mail: nhattori@hiroshima-u.ac.jp

doi: 10.1158/1535-7163.MCT-13-0041

©2013 American Association for Cancer Research.

To pursue the possibility that PAI-1 could be a therapeutic target in the management of malignancy, we first examined the effect of systemic administration of SK-216, a specific inhibitor for PAI-1, on tumor progression and angiogenesis. In this experiment, PAI-1-secreting Lewis lung carcinoma (LLC) cells and PAI-1-nonsecreting B16 melanoma cells were used to establish a subcutaneous tumor model and a tail vein metastasis model. Then, we determined whether host or tumor PAI-1 was more important in tumor progression and angiogenesis. Toward that end, we stably transfected LLC cells with short hairpin RNA (shRNA) to generate siRNA targeting PAI-1 (PAI-1-siRNA) or nonspecific scrambled siRNA (NS-siRNA), thereby yielding PAI-1 knockdown LLC (siPAI-1 LLC) cells or control LLC (siControl LLC) cells. After siPAI-1 LLC cells or siControl LLC cells were transplanted into PAI-1^{-/-} mice or wild-type (WT) mice, the degrees of tumor progression and angiogenesis were analyzed.

Materials and Methods

Cells and cell culture

LLC, B16 melanoma, and human embryonic kidney 293 cells were purchased from and authenticated by American Type Culture Collection. These cell lines were cultured in Dulbecco's Modified Eagle Medium (DMEM) supplemented with 10% FBS and 1% penicillin-streptomycin. Human umbilical vein endothelial cells (HUVEC) authenticated by Lifeline Cell Technology were purchased from Kurabo and cultured following the manufacturer's protocol. All cells were incubated at 37°C in a 5% CO₂ incubator and used within 6 months after resuscitation.

Reagents and animals

Matrigel was purchased from BD Biosciences. VEGF was obtained from Kurabo. SK-216 (Supplementary Fig. S1) was chemically synthesized and supplied by Shizuoka Coffein Co., Ltd.. Inhibitory activity of SK-216 on PAI-1 was investigated using previously published methods (24) and the IC₅₀ was determined to be 44 μmol/L as reported in international patent WO04/010996. Breeding pairs of the homozygous PAI-1^{-/-} mouse strain on a C57BL/6 background were purchased from The Jackson Laboratory. Age- and sex-matched WT C57BL/6 mice were purchased from the Charles River Laboratories. Animals were maintained according to guidelines for the ethical use of animals in research at Hiroshima University (Hiroshima, Japan).

Preparation of LLC cells stably expressing PAI-1-siRNA or NS-siRNA

To stably express siRNA in LLC cells, we used an shRNA expression vector containing a neomycin-resistant gene: pSINsi-mU6 (TaKaRa). Synthetic oligonucleotides to express shRNA were annealed and ligated into the linearized pSINsi-mU6 vector. The sequences of the oligonucleotides for shRNA to generate PAI-1-siRNA and

NS-siRNA were as follows: 5'-GATCCGCCAACAA-GAGCCAATCACATAGTGCTCCTGGTTGTGTGATTG-GCTCTTGTGGCTTTTTTAT-3' and 5'-GATCCGCT-TTAATCGCGTATAAGGCTAGTGCTCCTGGTTGGCC-TTATACGCGATTAAGACTTTTTTAT-3', respectively. These pSINsi-mU6 cassette vectors were transfected into 293 cells by the use of Retrovirus Constructive System Eco (TaKaRa), and the recombinant retroviral vectors containing the expression cassettes of PAI-1-siRNA and NS-siRNA were collected. These retroviral vectors were infected into LLC cells and followed by selection with G418 (Promega), LLC cells stably expressing PAI-1-siRNA or NS-siRNA (siPAI-1 or siControl LLC cells, respectively) were prepared.

Quantitative real-time PCR

Total RNA was isolated with RNeasy Mini Kits (Qiagen). The isolated total RNA was reverse transcribed into cDNA using a High Capacity RNA-to-cDNA Kit (Applied Biosystems) following the manufacturer's instructions. Quantitative real-time PCR (qRT-PCR) was conducted on an ABI Prism 7700 (Applied Biosystems) for mouse PAI-1 using β-actin as a control housekeeping gene.

Quantification of PAI-1 protein

Total PAI-1 secreted into culture medium for 24 hours was measured using an ELISA kit (Innovative Research) following the manufacturer's instructions. The minimum detection limit of this ELISA kit was 0.02 ng/mL.

Immunohistochemical staining of PAI-1

Immunohistochemical analysis of PAI-1 was conducted as described in the Supplementary Materials and Methods.

Subcutaneous tumor model

The indicated cells (1×10^6) were subcutaneously inoculated in the left flank of mice. For SK-216 experiments, the mice were given drinking water containing or lacking SK-216 (100 or 500 ppm). Until 14 days after the inoculation, the length and width of the tumors were measured using a caliper twice a week and tumor volume was calculated using the formula: width² × length × 0.5 (25).

Tail vein metastasis model

The indicated cells (3×10^5) were injected into mice through the tail vein. For SK-216 experiments, the mice were given drinking water containing or lacking SK-216 (100 or 500 ppm). Mice were euthanized 21 days after the cell injection and the number of grossly identified tumor nodules on the surfaces of the lungs was manually counted.

Evaluation of microvessel density in subcutaneous tumors

Tumor sections were incubated with a rabbit polyclonal antibody against mouse CD31 (Abcam) followed by 30-minute reaction with a biotinylated goat anti-rabbit immunoglobulin G (IgG) antibody (Vector Laboratories).